

GEOLOGI FOR SAMFUNNET

GEOLOGY FOR SOCIETY



Report no.: 2012.041		ISSN 0800-3416	Grading: Open
Title: Calculation of slope angle from bathymetry data using GIS – effects of computation algorithm, data resolution and analysis scale			
Authors: Margaret F.J. Dolan		Client: MAREANO	
County:		Commune:	
Map-sheet name (M=1:250.000)		Map-sheet no. and -name (M=1:50.000)	
Deposit name and grid-reference:		Number of pages: 44	Price (NOK): 165,-
		Map enclosures:	
Fieldwork carried out:	Date of report: 7 th August 2012	Project no.: 311702	Person responsible: <i>Reidun Bør</i>
<p>Summary:</p> <p>This report presents the results of a spatially nested case study using MAREANO multibeam bathymetry and regional data. The purpose of the case study was to investigate and illustrate common factors affecting terrain variables derived from multibeam bathymetry data – computation algorithm, data resolution and analysis scale. Slope was selected as the focus of this study as it is one of the most commonly used variables, and also the most intuitive to illustrate. This study examines the effects of computation algorithm, data resolution, and analysis scale on slope values computed in a geographic information system (GIS) environment. The results of the study are discussed in relation to geomorphology and benthic habitat mapping which are key components of Norway's MAREANO seabed mapping programme (www.mareano.no).</p>			
Keywords: Marine geology	MAREANO	Analysis scale	
Slope	Multibeam bathymetry	GIS	
Terrain variables	Geomorphology	Benthic habitat mapping	

CONTENTS

- 1. INTRODUCTION..... 7
- 2. CASE STUDY 8
 - 2.1 Slope calculation algorithm 10
 - 2.2 Data resolution and analysis scale 19
 - 2.2.1 Change resolution..... 21
 - 2.2.2 Average depth over $n \times n$ windows then calculate..... 22
 - 2.2.3 Calculate then average result over $n \times n$ windows 24
 - 2.2.4 Calculate at multiple scales using selected $n \times n$ analysis windows 26
 - 2.2.5 Multiscale analysis 28
 - 2.3 Other issues related to of slope calculations from bathymetry data 29
 - 2.3.1 Broad scale slope from Regional data vs. Multibeam data 29
 - 2.3.2 Effects of bathymetry data artefacts on slope calculations 31
 - 2.3.3 Detection of geomorphic structures and relevance to habitats..... 35
- 3. DISCUSSION AND CONCLUSIONS..... 37
 - 3.1 Computation algorithms 37
 - 3.2 Data resolution/analysis scale..... 38
 - 3.3 Other issues..... 39
 - 3.4 Conclusion 39
- 4. REFERENCES 41

FIGURES

Figure 1: Overview bathymetry map showing nested study area. The boundaries of the 1000 x 1000 km and 100 x 100 km study boxes are shown (white). Smaller study boxes lie within the 100 km box, these are shown in Figure 2. Map projection UTM 33N (WGS84)

Figure 2: Showing detailed 5 m multibeam bathymetry within the 10 x 10 km study area. 1 x 1 km boxes (white) are shown around the geomorphic features investigated further in this report: A – crystalline bedrock on continental shelf, B – iceberg ploughmarks on continental shelf, C – small canyon on upper continental slope. 100 x 100 m boxes (blue) are shown for A and B where more geomorphology and slope are examined in finer detail. Map projection UTM 33N (WGS84)

Figure 3: Visual summary of slope calculations on a 5 m grid using $n = 3$ using selected algorithms. Slope is shown as a semitransparent layer over shaded relief. Points A, B, C show the positions of sites for value extraction (Figures 4 – 7)

Figure 4: Summary of slope calculation values (degrees) using $n = 3$ on a 5 m bathymetry grid from different algorithms (Table 1) on different types of terrain (Figure 2)

Figure 5: Slope calculation values (degrees) using $n = 3$ on a 5 m bathymetry grid from different algorithms (Table 1) on different types of terrain (Figure 2). (a) crystalline bedrock; (b) iceberg ploughmarks; (c) canyon

Figure 6: Summary of slope calculation values (degrees) using $n = 3$ on a 50 m bathymetry grid from different algorithms (Table 1) on different types of terrain (Figure 2).

Figure 7: Slope calculation values (degrees) using $n = 3$ on a 50 m bathymetry grid from different algorithms (Table 1) on different types of terrain (Figure 2). (a) crystalline bedrock; (b) iceberg ploughmarks; (c) canyon

Figure 8: Illustration of edge effects from slope calculations using $n = 3$ on a 50 m resolution bathymetry. (a) spurious slope values at edge cells induced by use of temporary average value beyond the real data extent by ArcGIS - most obvious is the lower slope values (green) to the north of the image. (b) Null value assigned to outermost cell by Jenness where hillshade bathymetry can be seen underneath the slope layer showing the actual bathymetric data coverage.

Figure 9: Example of single-scale ($n = 3$) slope at three different cell sizes (a) 5 m, (b) 50 m, (c) 500 m. Note, the same colour scale is used for slope values across each cell size.

Figure 10: Variation in slope values calculated for 3 points from 5 m, 50 m, and 500 m bathymetry data. Calculations performed in ArcGIS ($n = 3$). Locations for extracted slope values from Figure 2.

Figure 11: Profile view of 5 m resolution bathymetry indicating approximate length scale (blue bars) over which a 3 x 3 cell analysis window operates about a point (red dot) for different data resolutions: 5 m (lowest bar), 50 m (middle bars), 500 m (uppermost bars). The location of the red dot roughly corresponds to the point used to extract slope values in Figure 2. Three examples are given to show the effect of the window size across varying types of terrain (a) crystalline bedrock on outer continental shelf (b) iceberg ploughmarks on continental shelf (c) small canyon on upper continental slope.

Figure 12: Illustrating the effect of averaging bathymetry over successively large window sizes prior to slope calculations. Computations based on 5 m bathymetry. Bathymetry averaged using Neighbourhood tools in ArcGIS Spatial Analyst using (a) $n = 9$; (b) $n = 21$; (c) $n = 49$. Slope calculated in ArcGIS using $n = 3$. The black and white ovals in (c) are for comparison with Figure 13.

Figure 13: Illustrating the effect of averaging slope calculations over successively large analysis window sizes. Computations based on 5 m bathymetry and initial slope calculation using ArcGIS ($n = 3$). Slope averaged using Neighbourhood tools in ArcGIS Spatial Analyst using (a) $n = 9$; (b) $n = 21$; (c) $n = 49$. The black oval shows the iceberg ploughmarks area with generally higher slopes in (c) than Figure 12 (c). The white oval shows where the area of broader slope is more similar to that in Figure 12 (c) but is lower than that for the iceberg ploughmarks area when average slope is used.

Figure 14: Illustrating the effect of calculating slope from bathymetry data directly using successively large analysis window sizes. Computations based on 5 m bathymetry using Landserf software with (a) $n = 5$; (b) $n = 7$; (c) $n = 9$; (d) $n = 21$; (e) $n = 49$.

Figure 15: Multiscale slope computed using $N = 49$ (i.e. $n = 3$ to 49). (a) mean slope over all analysis scales (b) standard deviation of slope over all analysis scales.

Figure 16: (a) Regional bathymetry 500 m resolution within a 1000 x 1000 km box (b) slope map calculated from regional bathymetry using ArcGIS ($n = 3$).

Figure 17. Bathymetry data at 500 m resolution within a 100 x 100 km box, based on (a) regional data (b) multibeam data. Bathymetry data are shown together with derived slope maps calculated in ArcGIS ($n = 3$) (c) slope from regional bathymetry (d) slope from multibeam

Figure 18: Illustrating artefacts in multibeam data in the vicinity of each 1 x 1 km test site (a) rock, (b) ploughmarks, (c) canyon. Artefacts are visible as strips (corrugations) in the

hillshaded bathymetry and are highlighted by erroneous slope values, the orientation of artefacts is indicated at selected locations by double headed arrows

Figure 19: Slope calculations using a selection of approaches from Table 1 to see the effect on overcoming artefacts in the bathymetry dataset. The 1 x 1 km box at the canyon on the upper continental slope (site C – Figure 2) and surrounding neighbourhood are shown. Example artefact locations are indicated by arrows.

Figure 20: Showing slope calculated from 5m resolution bathymetry data using ArcGIS ($n = 3$) within the neighbourhood of a 100m² box (black) in the rocky study area. Point observations of sediment cover from a towed video transect are overlain on the slope map, so show how the variation in sediments (often linked to habitats) varies with slope in this area.

TABLES

Table 1: Summary of the slope calculation algorithms employed in this study.

Table 2: The five main approaches to obtaining terrain indices at different scales with a summary of the computations performed for this study to illustrate the effects of each approach.

1. INTRODUCTION

Bathymetric datasets around the world have improved significantly over the last couple of decades. On a global scale we have gained access to satellite bathymetry which has been used to complement other available bathymetry data and contribute to world data sets such as GEBCO (IOC, IHO and BODC 2003). Multibeam echosounder, or swath bathymetry data have become the standard for acoustic seabed mapping, both for hydrographic and other purposes such as geological mapping and habitat mapping. With the latest generation of multibeam systems, sounding data density has increased significantly, allowing detailed mapping of the bathymetry and morphology of the seabed, even in deep waters beyond the continental shelf.

Ship-borne bathymetric mapping in deeper waters uses low frequency echosounding systems with lower sounding density and resulting data resolution. Shallow water surveys using higher frequency multibeam systems can acquire very high resolution data, often sub-metre grids. When the same type of systems are mounted on underwater vehicles similarly high resolution data can be obtained in deep water when supported by good navigation and motion sensor information. In coastal waters airborne laser systems e.g. LIDAR provide an effective means to survey shallow waters in regions with sufficient water clarity providing one effective means to bridge the gap between marine and terrestrial topographic data.

While only a small percentage of the global ocean has been mapped with such methods to date, this technology has meant a dramatic leap in the knowledge of the morphology of the sea floor. Within the course of a single multibeam survey, bathymetry maps for a study area which were previously based on 19th century lead-line soundings can be updated to 100% coverage detailed digital terrain model (DTM) showing the detailed structure of the seabed morphology as well as giving accurate bathymetry for hydrographic purposes.

In the marine environment the arrival of modern bathymetry data has come at the same time as a dramatic rise in computing technology and the use of geographic information systems (GIS) in marine science. This has put new bathymetric data directly in the hands of scientists from a variety of disciplines, not just specialist cartographers making nautical charts or interpreted products. The impressive bathymetry data revealing the seabed and many previously unknown and impressive structures have breathed new life into investigations of the seabed. They have provided new data for management (Pickrill and Todd 2003) together with much of the impetus for many applied, cross disciplinary studies of the seafloor, not least benthic habitat mapping, as reviewed by Brown et al. (2011). This situation contrasts with terrestrial topographic data, where more gradual improvements have been made over time and there is a more complete history of improvements in digital elevation models (DEMs), see review by Wilson (2012). Associated with this, the derivation of terrain variables and interpretation of landforms from the data is traceable through the

geomorphological literature, see reviews by Evans (2012), Wilson (2012), and supported by relevant field observations, something that is difficult for marine studies to echo.

The terrestrial literature is also full of evaluation of different methods for terrain characterisation using quantitative terrain indices such as slope, curvature etc. (e.g. Evans 1972, Evans 1980, Evans 2012, Dragut et al. 2009, Florinsky 1998a, Florinsky 1998b, García Rodríguez and Giménez Suárez 2010, Grohmann et al. 2011, Hickey et al. 1994, Hickey 2000, Jones 1998, Shary, Sharaya and Mitusov 2002, Shi et al. 2007, Warren et al. 2004, Wilson 2012, Zhang et al. 1999). Much of this literature is directly relevant to bathymetry data and the majority of computation methods can be adopted equally well for bathymetric data, with regard for similar key issues – data resolution, computation algorithms, analysis scale. However, despite the fact that bathymetric data and GIS-based terrain analysis have been widely used for at least the last decade there remains a small volume of literature specifically focusing on the computation and use of terrain variables in a marine context. This gap is important since there are several issues that are particular to bathymetric data, particularly multibeam data, including data acquisition artefacts and data resolution linked to the technology available for surveying at different depths. Slope was selected as the basis for this study, and represents just one example of a terrain variable that may be derived from bathymetry data. Many of the discussion points will be equally relevant to other bathymetrically derived terrain variables e.g. aspect, curvature, terrain variability (*sensu* Wilson et al. 2007) but in this study each key issue will be examined in turn with reference to slope calculations performed on an example data set. The emphasis in this study is on visual comparison of results as these are most intuitive to interpret.

Whilst it serves as an example terrain variable in this report to examine the key issues, slope is important in its own right, particularly in relation to benthic habitat. Slope is relevant in a geomorphological context due to its inherent link to the stability of sediments and hence to grain size. Slope is also linked to local acceleration of currents which relates to erosion, movement of sediments, and the creation of bedforms. Slope also has ecological relevance where its link to the stability of sediments affects the ability of bottom-dwelling animals to live in/on sediments. In an ecological sense the local acceleration of currents is related to food supply and exposure for benthic fauna.

2. CASE STUDY

The case study presented here uses multibeam data from the Norwegian offshore seabed mapping programme, MAREANO, together with a regional bathymetric dataset provided by the Norwegian Hydrographic Service which comprises data from various sources. The multibeam data have been gridded at 5 m (fine scale), 50 m (intermediate resolution) and 500 m (regional resolution) to illustrate various issues associated with the data and slope calculations. The regional bathymetric data were available only at 500 m resolution; this is

the same resolution as bathymetry data recently available through the EMODNET Hydrography Portal for much of Europe (<http://www.emodnet-hydrography.eu/>). Although the study area is outside the current limits of EMODNET coverage, data at this resolution from compiled data sources will be increasingly used in national and pan-European studies.

The key issues associated with slope calculations will be investigated within a nested case study in the Nordland VII area, North Norway (Figures 1, 2). In this area the MAREANO multibeam data coverage is extensive enough to cover most of a 100 x 100 km box.

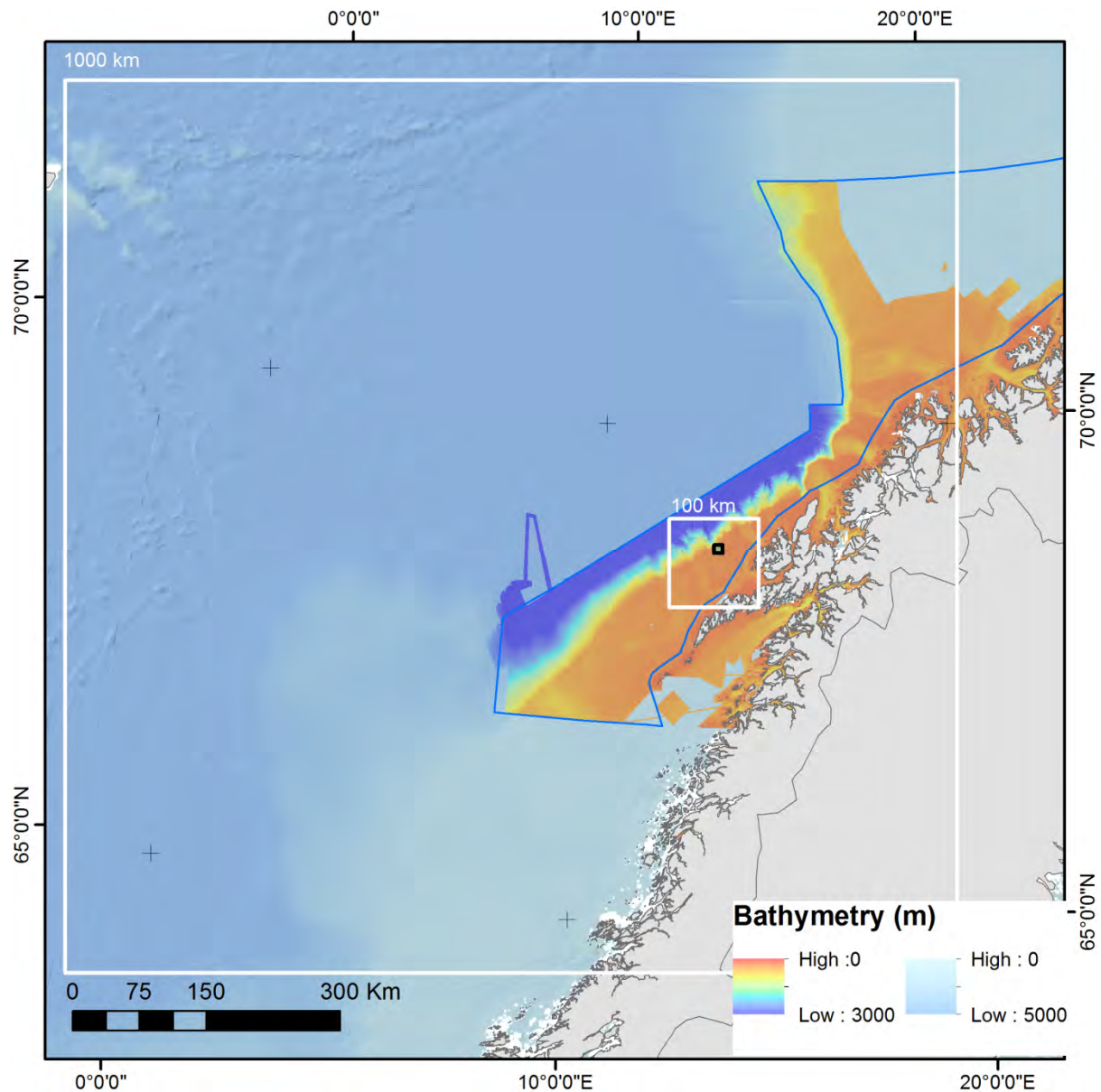


Figure 1. Overview bathymetry map showing nested study area. The boundaries of the 1000 x 1000 km and 100 x 100 km study boxes are shown (white). Smaller study boxes lie within the 100 km box, these are shown in Figure 2. Map projection UTM 33N (WGS84).

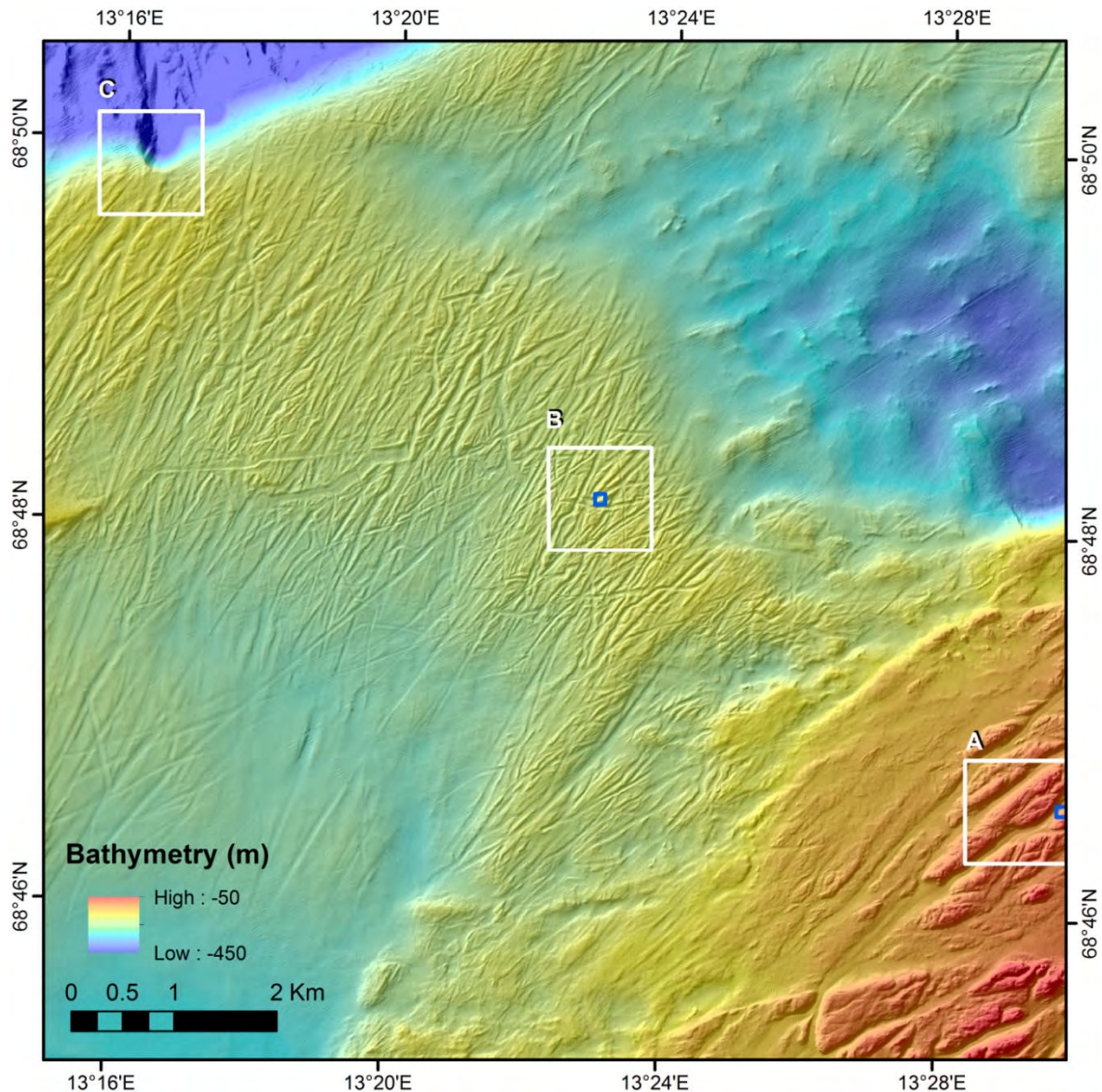


Figure 2. Showing detailed 5 m multibeam bathymetry within the 10 x 10 km study area. 1 x 1 km boxes (white) are shown around the geomorphic features investigated further in this report: A – crystalline bedrock on continental shelf, B – iceberg ploughmarks on continental shelf, C – small canyon on upper continental slope. 100 x 100 m boxes (blue) are shown for A and B where more geomorphology and slope are examined in finer detail. Map projection UTM 33N (WGS84).

2.1 Slope calculation algorithm

Calculation of terrain variables requires some method for mathematically representing the topographic surface and then using this to calculate the required terrain variable. Surface representation is typically achieved by either using neighbourhood analysis of raster pixels, where n = number of cells in the neighbourhood, or by fitting a polynomial expression to

describe the surface, or digital terrain model. Slope, or other terrain variable value, is then calculated for each raster pixel in turn using a specified computation algorithm. A great many methods have been proposed in the literature for the calculation of slope. Some terrestrial studies have compared results from the various methods for slope calculation (e.g. Dunn and Hickey 1998, Gao et al. 2012, García Rodríguez and Giménez Suárez 2010, Hickey 2000, Hodgson 1995) but based on the published literature it appears that the issue has not been investigated specifically for bathymetry data.

For this study, slope algorithms readily available in GIS and related software have been selected, focussing on those which are in common use, or easily accessible for those involved in seabed mapping. This includes commercial (ArcGIS, Fledermaus) and freely available software and tools for ArcGIS (Landserf, Jenness, SEXTANTE) developed in academia. The algorithms and software are summarised in Table 1.

Table 1. Summary of the slope calculation algorithms employed in this study.

Software	Method
ArcGIS v10 Spatial Analyst	Horn 1981
Landserf v3.2 (Wood 2009)	Wood [Evans (1980)]
Fledermaus DMagic v7.3.1	'Simple'
	'Balanced'
	Fitted (Horn 1981)
Jenness Surface tools for ArcGIS (Jenness 2011)	'Four cell'
	Horn (1981)
	Sharpnack & Akin (1969)
SEXTANTE for ArcGIS (Olaya, 2011)	Travis et al. (1975)
	Tarboton (1997)
	Costa-Cabral & Burgess (1996)
	Bauer et al. (1985)
	Heerdegen & Beran (1982)
	Zevenbergen & Thorne (1987)
	Haralick (1983)

The effect of using different slope calculation algorithms was examined using data in the 10 x 10 km study area as it presents the best opportunity to visualise the results. The effects of the computation algorithms were tested on 5 m and 50 m bathymetry grids at each of the sites A-C shown in Figure 1. The results are summarised in Figures 3 to 9. Figure 3 shows a visual summary of a selection of the different algorithms, using a consistent colour scheme across all slope grids where some differences can be seen between the values calculated and the features highlighted by them. Slope values from the indicated sites A (rock), B (ploughmarks) and C (canyon) are summarised in the graphs showing the results of slope calculations at different resolutions.

From Figures 4 to 7 it can be seen that many of the algorithms give similar values, at a particular resolution, however, there can be quite a difference in the range of values generated, depending on the algorithm used. The effect of the algorithm used on values generated varies with the resolution of the bathymetry data used for slope calculations, and also with the type (scale) of the terrain features present. We see that the Haralick (1983) algorithm is consistently distinct from the other methods and appears the most unstable. It produces a lower slope value than the other algorithms for all features when calculations are made using the 5 m bathymetry grid. Using the 50 m bathymetry grid however, the Haralick (1983) method consistently overestimates the slope value for all feature types.

Most of the other algorithms are more stable and give more comparable results, however it can be seen that several of the algorithms underestimate the slope, particularly for small features (iceberg ploughmarks) with Fledermaus (simple), Travis et al. (1975) and Tarboton (1997) all giving low values at this site, even using the 5 m grid (Figures 4, 5b). Examination of the results from the 50 m grid (Figures 6, 7b) shows that Fledermaus (simple) gives a high value at the same site, however both Travis' and Tarboton's methods give a low (zero) value, i.e. the site is seen as flat. The Fledermaus (balanced) algorithm also shows quite a degree of variation from the average results from the other algorithms, and the Jenness (4 cell) and Zevenbergen and Thorne (1987) algorithms are noticeably different with higher values for slopes over small features (ploughmarks). The rest of the algorithms largely agree within a few degrees, though it should be noted that the margin for error is smaller using the 50 m grid since all slope values are lower.

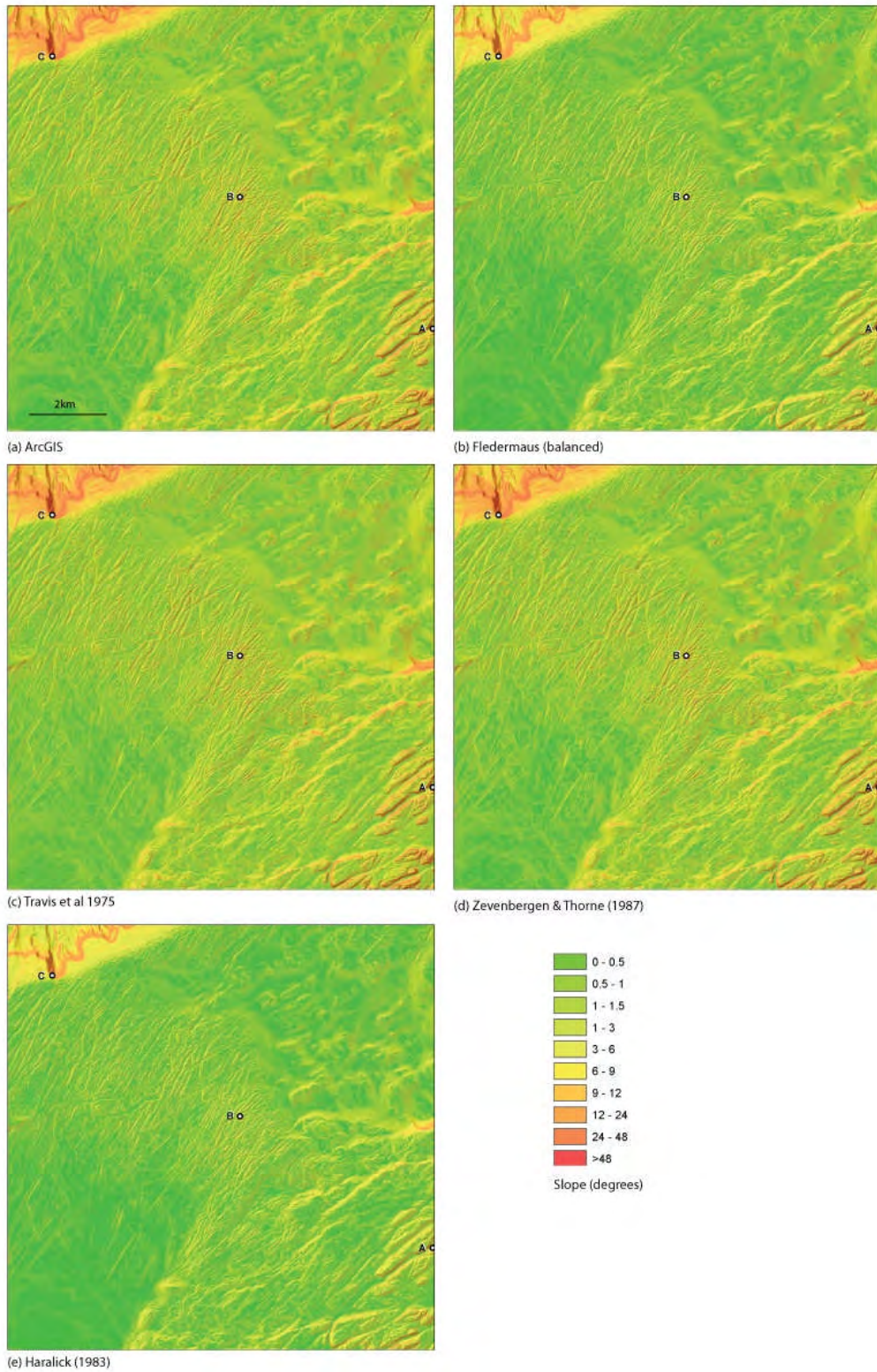


Figure 3. Visual summary of slope calculations on a 5 m grid using $n = 3$ and selected algorithms. Slope is shown as a semitransparent layer over shaded relief. Points A, B and C show the positions of sites for value extraction (Figures 4-7).

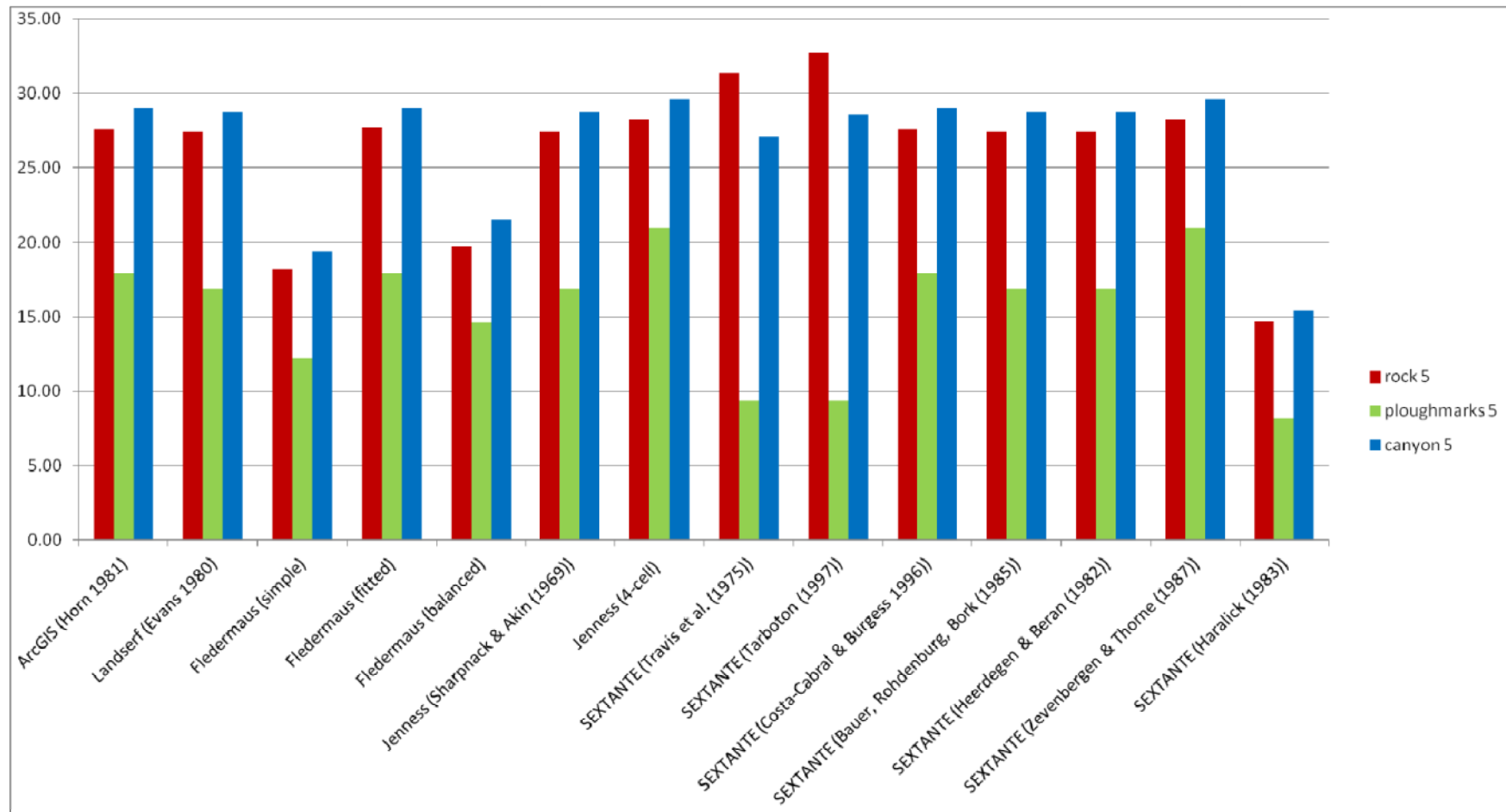


Figure 4. Summary of slope calculation values (degrees) using $n = 3$ on a 5 m bathymetry grid from different algorithms (Table 1) on different types of terrain (Figure 2).

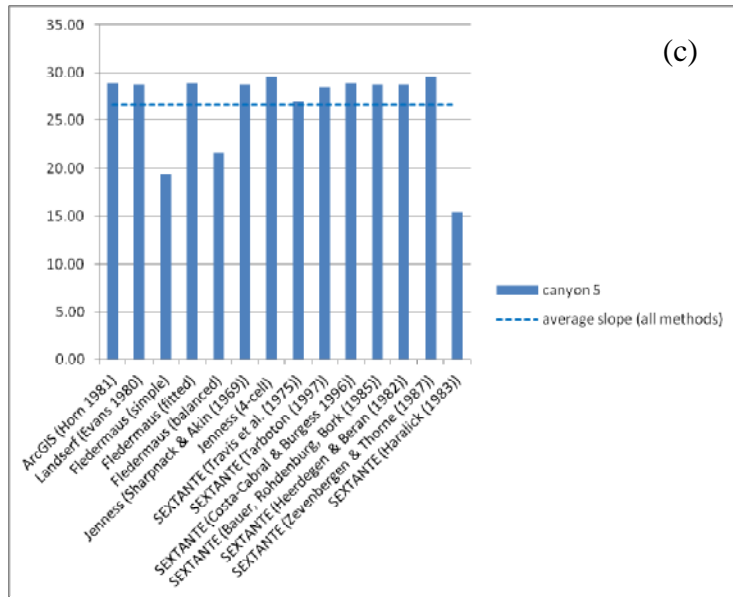
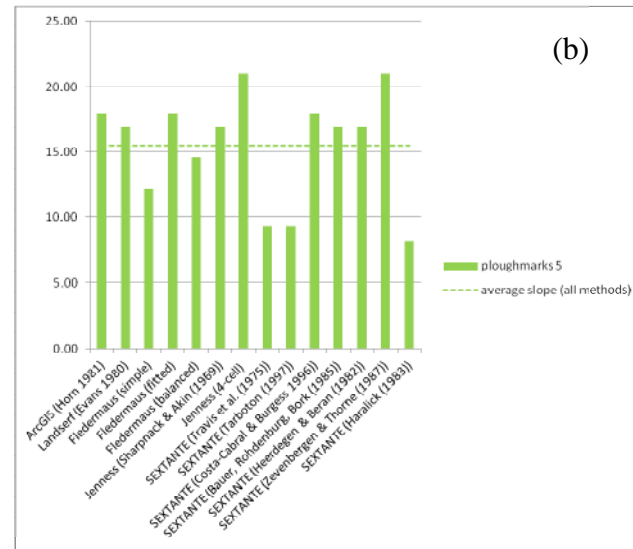
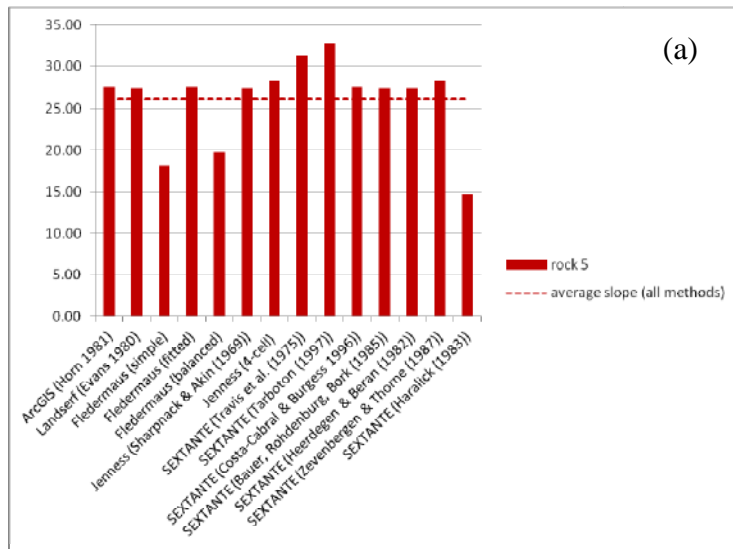


Figure 5. Slope calculation values (degrees) using $n = 3$ on a 5 m bathymetry grid from different algorithms (Table 1) on different types of terrain (Figure 2). (a) crystalline bedrock; (b) iceberg ploughmarks; (c) canyon.

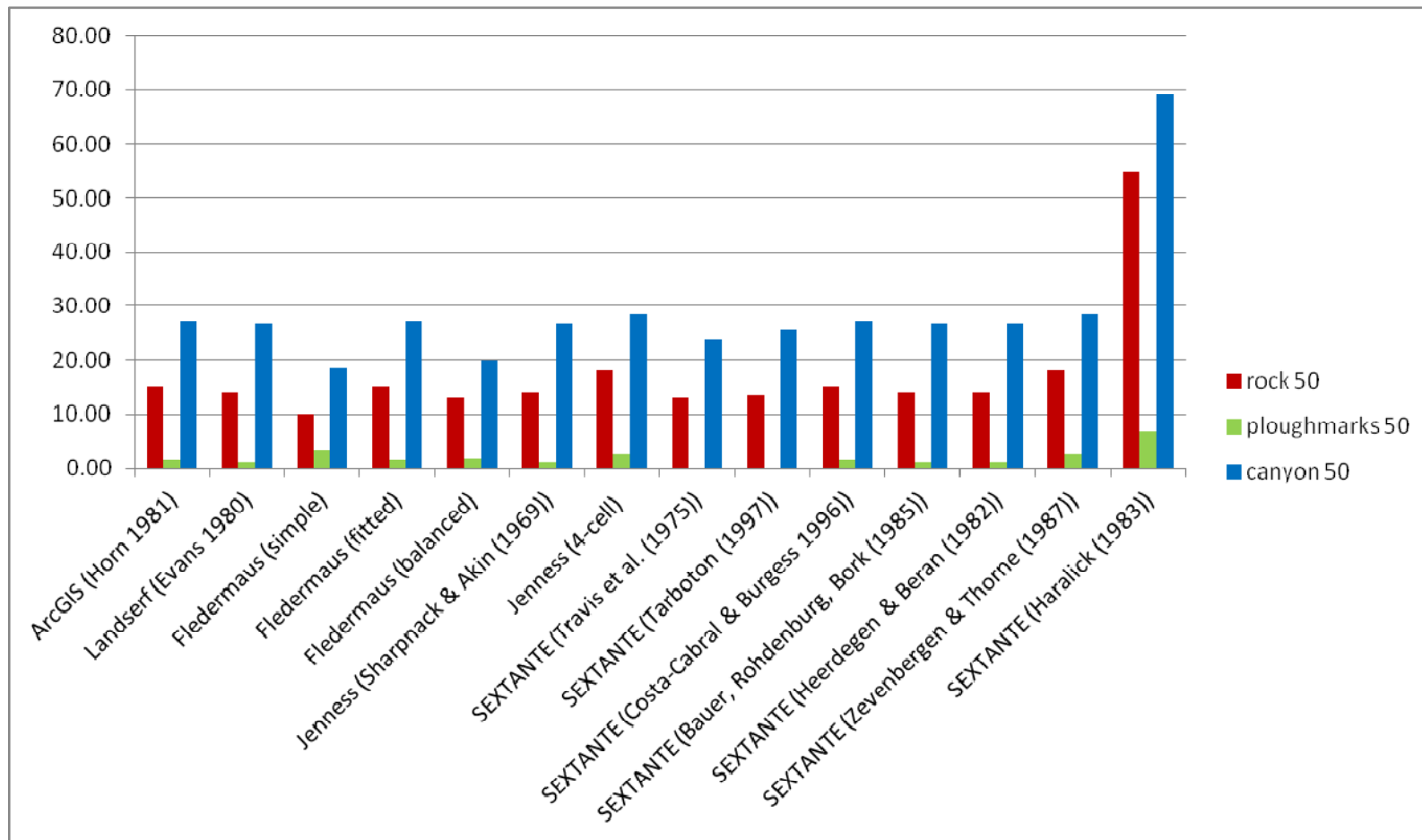


Figure 6. Summary of slope calculation values (degrees) using $n = 3$ on a 50 m bathymetry grid from different algorithms (Table 1) on different types of terrain (Figure 2).

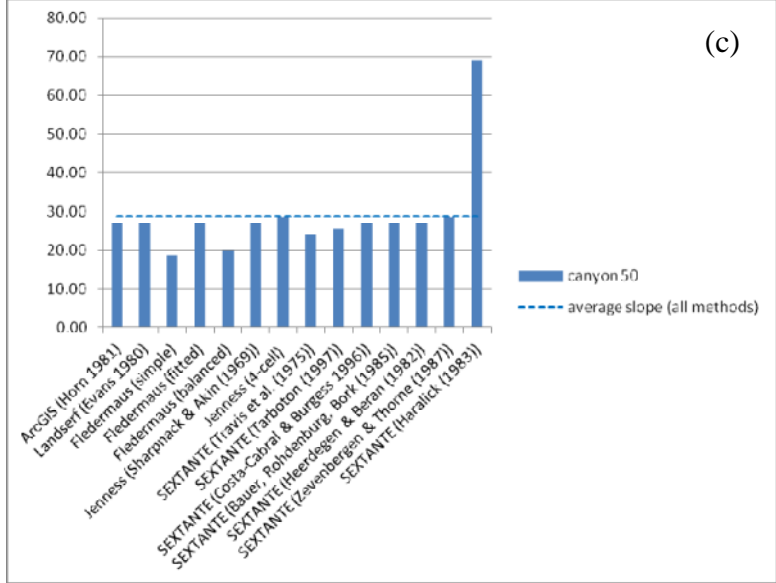
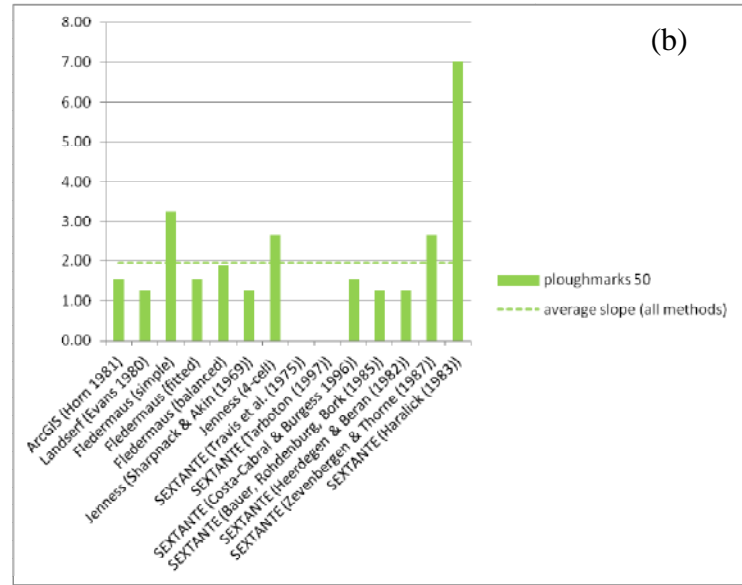
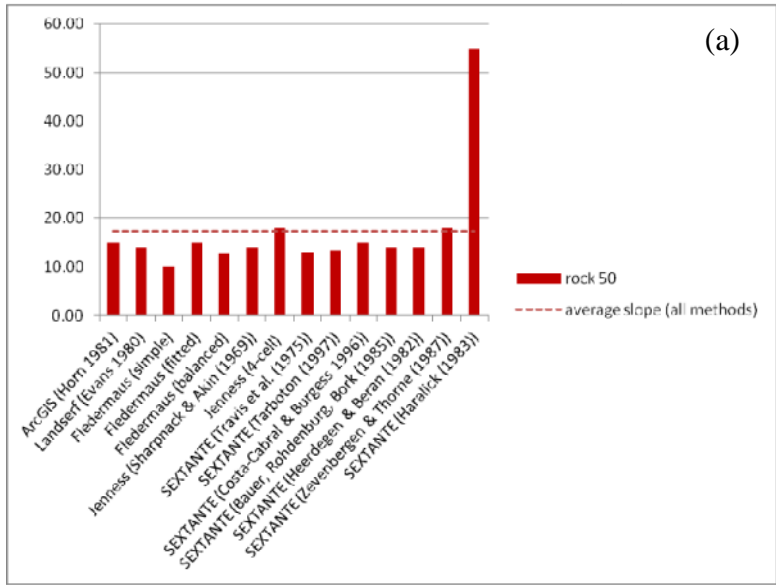


Figure 7. Slope calculation values (degrees) using $n = 3$ on a 50 m bathymetry grid from different algorithms (Table 1) on different types of terrain (Figure 2). (a) crystalline bedrock; (b) iceberg ploughmarks; (c) canyon.

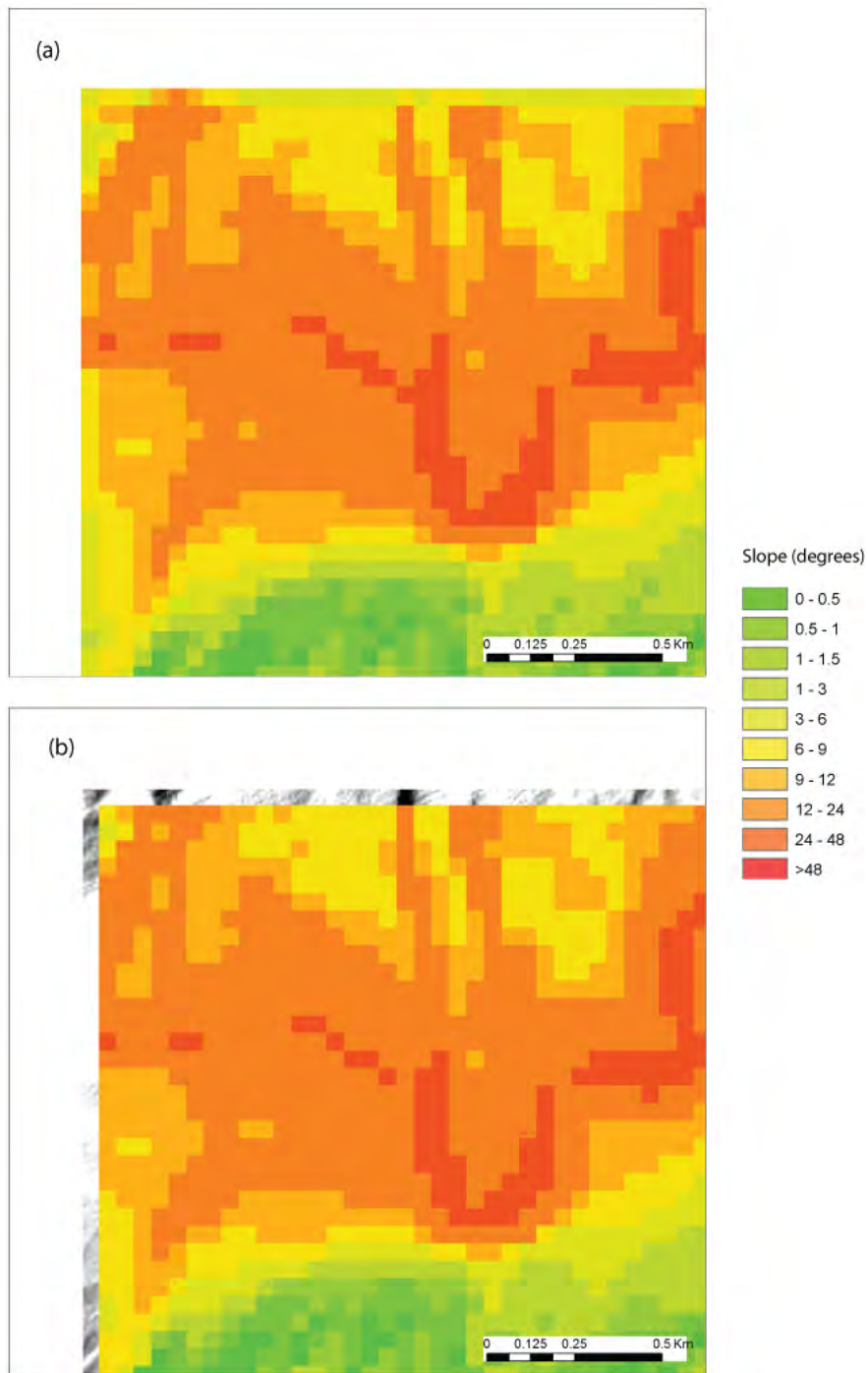


Figure 8. Illustration of edge effects from slope calculations using $n = 3$ on a 50 m resolution bathymetry. (a) Spurious slope values at edge cells induced by use of temporary average value beyond the real data extent by ArcGIS - most obvious is the lower slope values (green) to the north of the image. (b) Null value assigned to outermost cell by Jenness, where hillshade bathymetry can be seen underneath the slope layer showing the actual bathymetric data coverage.

The Fledermaus fitted algorithm is exactly the same as Horn's (1981) algorithm implemented in ArcGIS. Note also that the Jenness (2011) implementation of Horn's (1981) algorithm is essentially the same as that available in ArcGIS. However there is an important difference at the edge of the dataset. ArcGIS (and Fledermaus) implementations of Horn's (1981) algorithm induce edge effects as a temporary cell is created (based on average values) outside the data to enable the outermost cell within the 3 x 3 neighbourhood window to be assigned a slope value. Jenness' (2011) implementation does not use this approach, it simply does not provide a slope value if the entire $n \times n$ pixel neighbourhood does not contain bathymetry data, and therefore the resulting slope grid does not contain a value at the outermost cell (as Landsferf (Wood, 2009)). Examples of the edge effects are shown in Figure 8 using the 50 m grid from an area on a broad steep slope where the effect is more obvious (see also section 3.2.2-3.2.5).

On a more practical note, when performing the calculations it was observed that calculations using any of the SEXTANTE-based methods took significantly longer than the other computations, taking several minutes for each slope calculation based on the 5 m grid as opposed to several seconds for the other methods in ArcGIS and other software. Computation time is an important consideration, especially when working with large datasets. It is possible that future versions of the SEXTANTE toolbox will improve processing time, which would improve the accessibility to use of the other algorithms offered within the toolbox.

2.2 Data resolution and analysis scale

It is difficult to separate these issues as they are intrinsically linked. The scale dependence of terrain variables is a '*basic problem in geomorphology*' (Shary et al. 2002) which has long been recognised in terrestrial geomorphology (Evans 1972). Shary et al. (2002) point out the motivation for finding 'scale free' morphometric variables (terrain variables) and provide several demonstrations of the changing values of variables with data resolution. The problem is no different when it comes to bathymetry data. The values of all terrain variables are dependent on the resolution of the raster bathymetry data from which they are derived, and the analysis scale over which they are calculated.

There are five main approaches to obtaining terrain indices at different scales which are summarised in Table 2. The computations performed for this study are also outlined to illustrate the effects of each approach.

Table 2. The five main approaches to obtaining terrain indices at different scales with a summary of the computations performed for this study to illustrate the effects of each approach.

Approach	Description	Calculation methods used in this study
1	Change resolution (resampling) then calculate terrain variable	5 m bathymetry data resampled to 50 m, 500 m and then slope calculated using ArcGIS Spatial Analyst (3 x 3 cell analysis window).
2	Average depth over $n \times n$ windows then calculate terrain variable	Focal Statistics tool in ArcGIS Spatial Analyst used to calculate the mean bathymetry within $n \times n$ analysis windows where $n = 9, 21, 49$.
3	Calculate terrain variable then average result over $n \times n$ window	Slope calculated using ArcGIS Spatial Analyst (3 x 3 cell analysis window) then Focal Statistics tool used to calculate the mean slope within $n \times n$ analysis windows where $n = 9, 21, 49$
4	Calculate terrain variable at multiple scales using selected $n \times n$ analysis windows	Slopes calculated at multiple $n \times n$ analysis windows where $n = 9, 21, 49$ using Landserf v2.3 software.
5	Multiscale analysis* of terrain variable	Multiscale slope calculated for $N = 49$, i.e. across a series of analysis windows from $n = 3$ to 49 using Landserf v2.3 software. Results report mean value of slope across all scales plus standard deviation in slope values across analysis scales.

* Note that Wilson et al. (2007) used the term multiscale analysis for all types of analysis beyond the 3 x 3 standard analysis window. For clarity we now adopt the term *multiple scale* analysis to refer to analysis at successive analysis window, while reserving the term *multiscale* analysis for analysis which runs concurrently at multiple scales and reports the mean value and standard deviation over all analysis scales considered. $n \times n$ refers to the size of the analysis window in raster grid cells where $n = 3, 9$, etc.

For ease of visualisation, each of these effects is examined in detail using data within the 10 x 10 km box. It is at this mapping scale and finer that most regional geological interpretation and related studies e.g. habitat mapping are performed. Zooming in on this area as far as a 100 m² box shows how the bathymetry data and computed slope correspond with seabed morphology and habitats. Note that the same colour scale is used for slope maps in all figures to aid comparison of results.

2.2.1 Change resolution

Using standard desktop GIS (e.g. ArcGIS) the variables are calculated using a 3 x 3 analysis window around each pixel in turn. For a 5 m raster bathymetry grid the distance over which slope is measured, for instance, would be 15 m x 15 m (3 x 5 m cells). Using a 50 m grid the slope would be measured over a distance of 150 m x 150 m, and using a 500 m grid this increases to 1500 m. Due to the different length scales considered, plus the level of detail of the bathymetry data, slope values for a particular location, based on each of these different datasets, will give very different results.

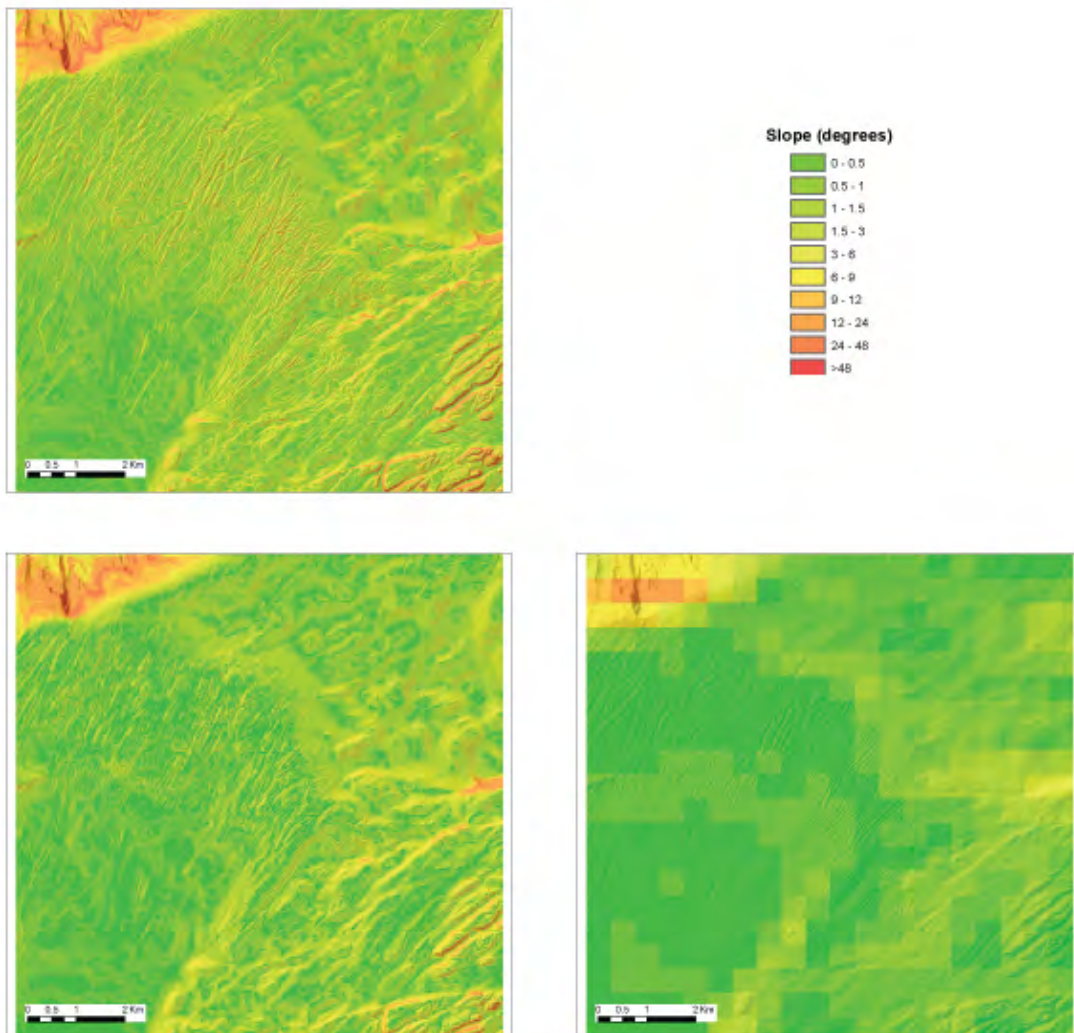


Figure 9. Example of single-scale ($n = 3$) slope at three different cell sizes (a) 5 m, (b) 50 m, (c) 500 m. Note, the same colour scale is used for slope values across each cell size.

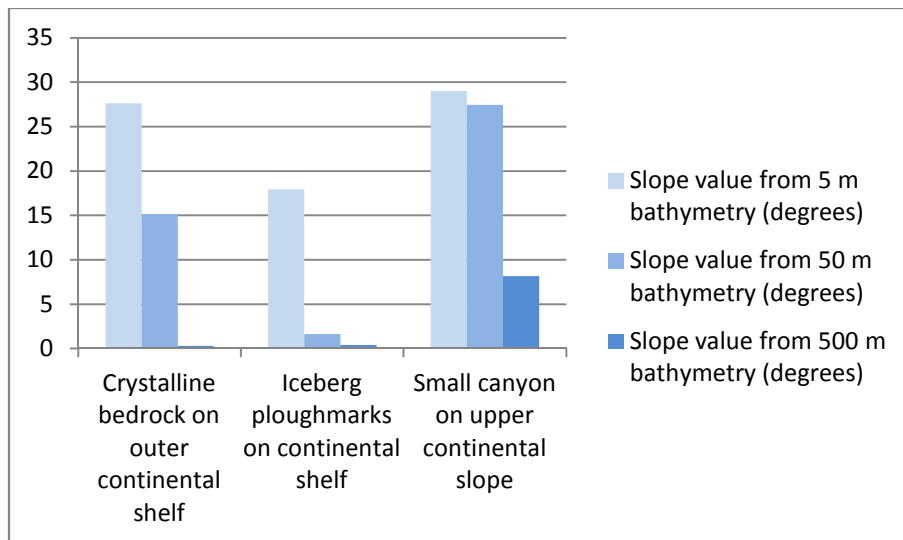


Figure 10. Variation in slope values calculated for 3 points from 5 m, 50 m and 500 m bathymetry data. Calculations performed in ArcGIS ($n = 3$). Locations for extracted slope values are shown in Figure 2.

An example is given in Figure 10 showing slope values for different sizes and types of geomorphic features (see Figure 2 for locations). Figure 11 shows profiles across the points shown in Figure 2 indicating the extent of the analysis window for each scale of computation. With the advent of easily generated slope values in desktop GIS it is all too easy to take the values generated by GIS slope calculation tools without thinking about what they really represent, and over which length scales.

2.2.2 Average depth over $n \times n$ windows then calculate

To test this approach bathymetry data (5 m) was averaged using the Neighbourhood tools in ArcGIS Spatial Analyst using (a) $n = 9$; (b) $n = 21$; (c) $n = 49$. The option ‘ignore NoData values in calculations’ was checked, with the result that a value for mean bathymetry is produced right to the edge of the bathymetry which is subsequently used in slope calculations (see discussion in section 2.1 on edge effects). Averaging the depth prior to slope calculation has the effect of smoothing the bathymetry data over which the slope is analysed. This may have benefits for data with artefacts, but real slopes associated with small structures may also be lost in the averaging process. Some examples are shown in Figure 12, where it can be seen how the small slopes associated with iceberg ploughmarks in the centre of the image become blurred when averaged using $n = 21$ and are no longer visible when $n = 49$ is used.

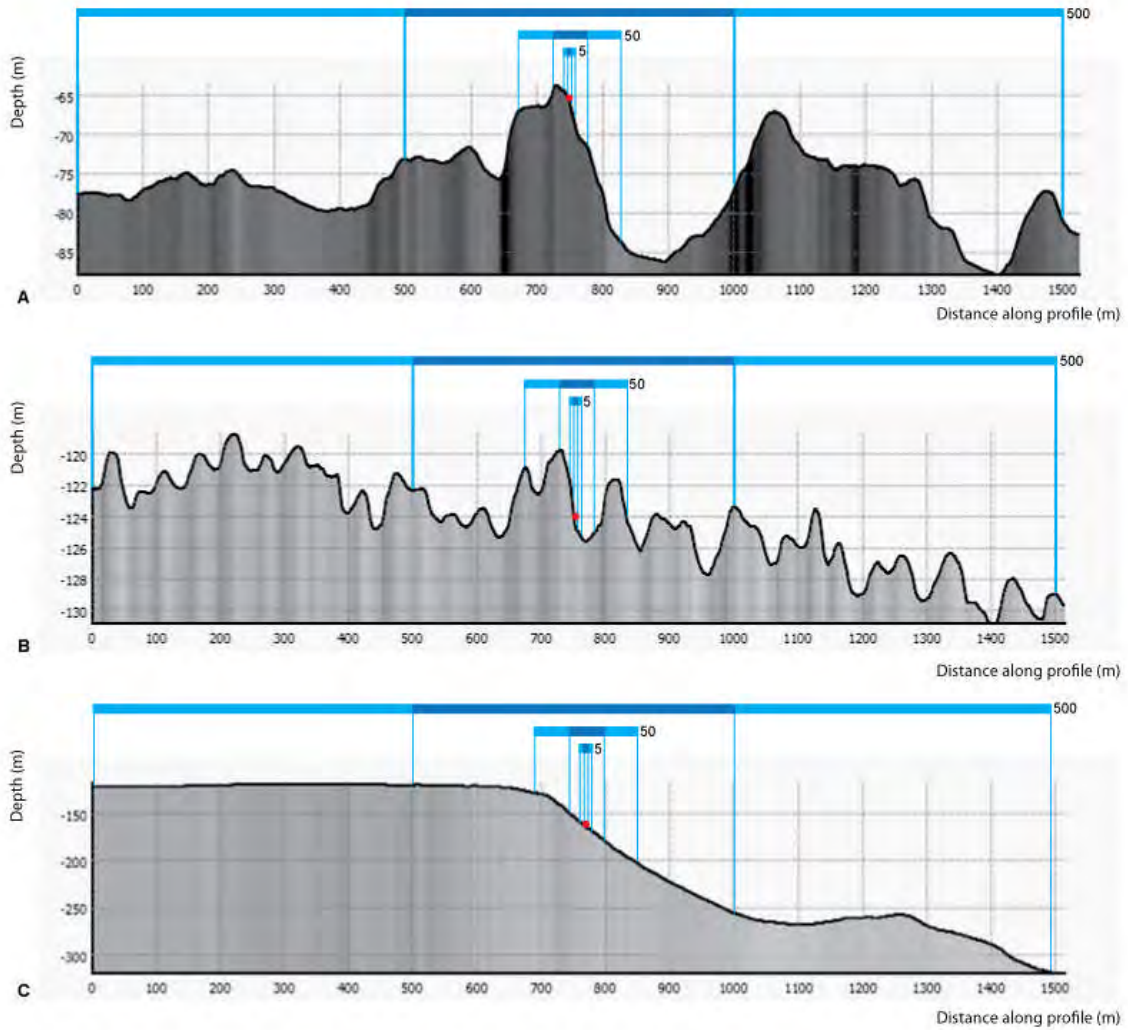


Figure 11. Profile view of 5 m resolution bathymetry indicating approximate length scale (blue bars) over which a 3 x 3 cell analysis window operates about a point (red dot) for different data resolutions: 5 m (lowest bar), 50 m (middle bars), 500 m (uppermost bars). The location of the red dot roughly corresponds to the point used to extract slope values in Figure 2. Three examples are given to show the effect of the window size across varying types of terrain; (A) crystalline bedrock on outer continental shelf, (B) iceberg ploughmarks on continental shelf, and (C) small canyon on upper continental slope.

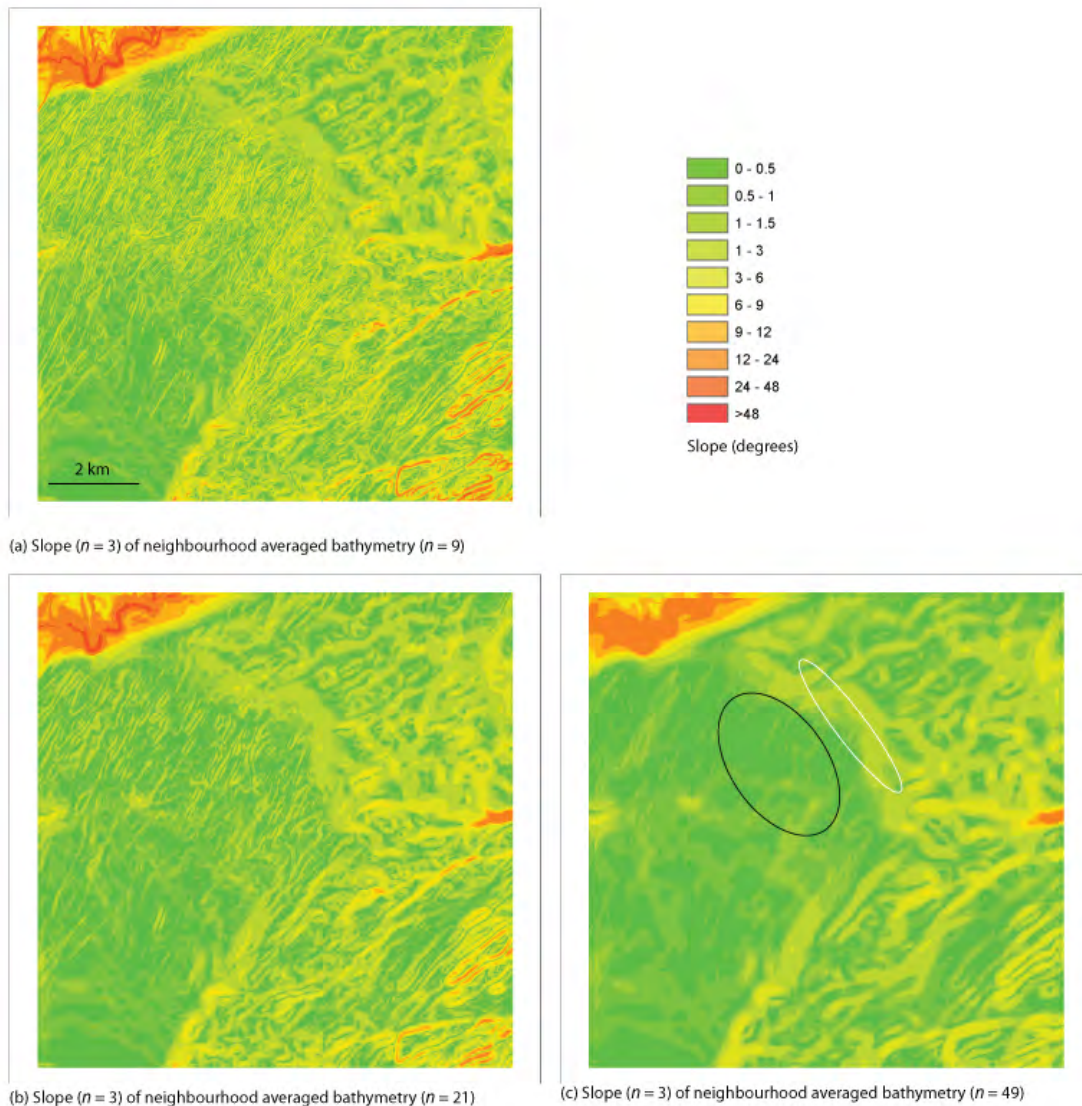


Figure 12. Illustrating the effect of averaging bathymetry over successively large window sizes prior to slope calculations. Computations based on 5 m bathymetry. Bathymetry averaged using Neighbourhood tools in ArcGIS Spatial Analyst using (a) $n = 9$; (b) $n = 21$; (c) $n = 49$. Slope calculated in ArcGIS using $n = 3$. The black and white ovals in (c) are for comparison with Figure 13.

2.2.3 Calculate then average result over $n \times n$ windows

To test this approach slope values were computed from bathymetry data (5 m) in ArcGIS using $n = 3$. The resulting slope grid was then averaged using the Neighbourhood tools in ArcGIS Spatial Analyst using (a) $n = 9$; (b) $n = 21$; (c) $n = 49$ to produce grids of average slope at successively large analysis window sizes (Figure 13). The option ‘ignore NoData values in calculations’ was unchecked this time, such that no value for mean slope was produced for a cell if its entire $n \times n$ neighbourhood is not full of data, resulting in null data values in the averaged slope grids near the edge of the data (see discussion in section 2.1 on

edge effects). Averaging the slope has a spatially similar effect to smoothing the bathymetry prior to slope calculation data, in terms of the level of detail visible with different n values, however comparing Figures 12 and 13 (noting that the same colour scale is used for slope in each figure) it can be seen that the values generated by the two approaches differ, and also that different terrain features are highlighted by the two approaches, especially at the larger window sizes ($n = 21, 49$).

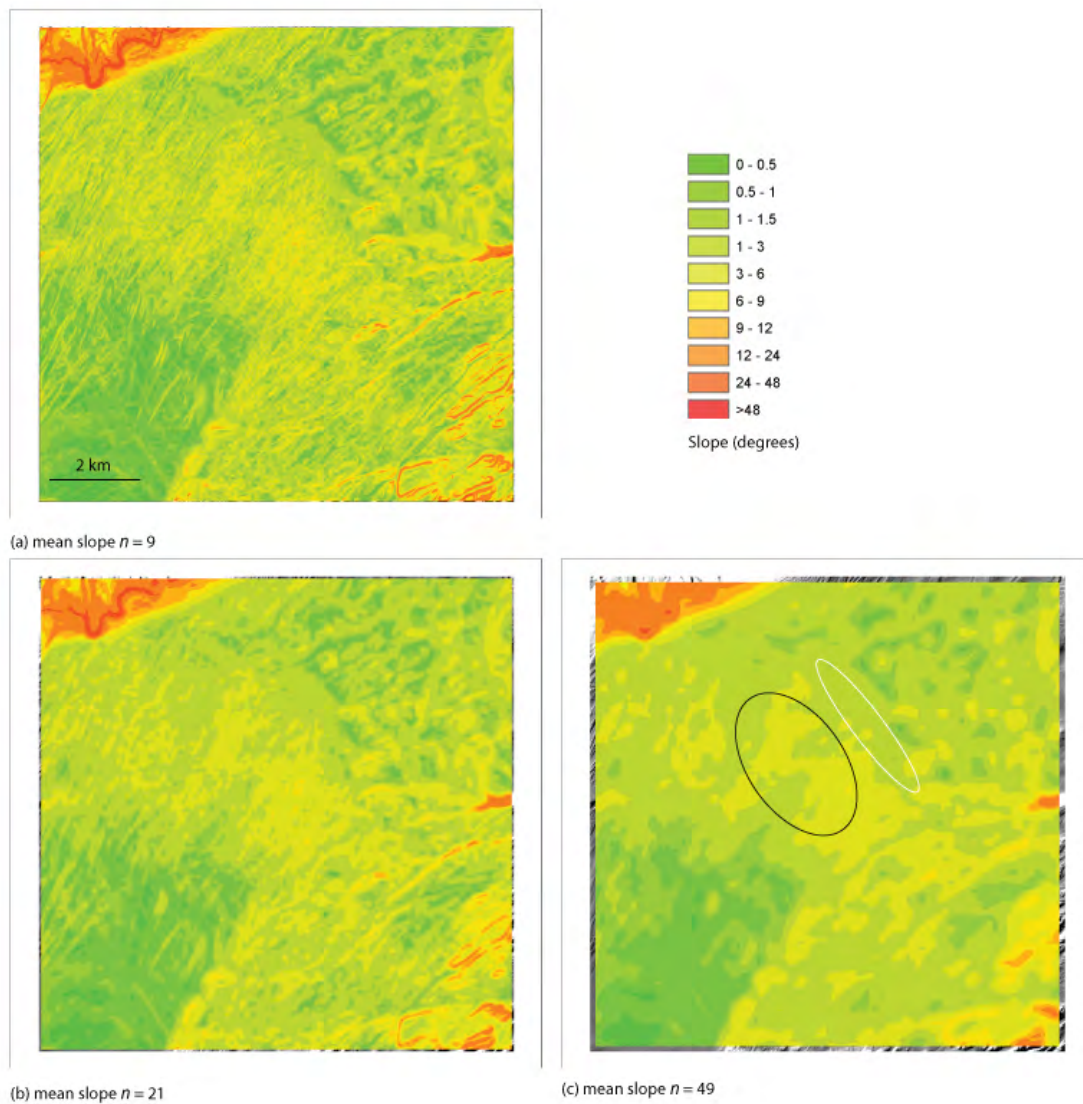


Figure 13. Illustrating the effect of averaging slope calculations over successively larger analysis window sizes. Computations based on 5 m bathymetry and initial slope calculation using ArcGIS ($n = 3$). Slope averaged using Neighbourhood tools in ArcGIS Spatial Analyst using (a) $n = 9$; (b) $n = 21$; (c) $n = 49$. The black oval shows the iceberg ploughmarks area with generally higher slopes in (c) than Figure 12 (c). The white oval shows where the area of broader slope is more similar to that in Figure 12 (c) but is lower than that for the iceberg ploughmarks area when average slope is used.

Averaging slope (Figure 13) produces generally higher slope values than averaging bathymetry before calculating slope (Figure 12) and also higher values than generated using lower resolution bathymetry (Figure 9). Figure 13 shows how the slope values over the iceberg ploughmarks in the centre of the image appear quite high when average slope is used, whereas the slope calculated from averaged bathymetry at the same location (Figure 12c – black oval) is quite low and higher slopes are indicated to the north east of this with values more similar to, although slightly higher than those from averaging bathymetry (Figure 12c – white oval).

2.2.4 Calculate at multiple scales using selected $n \times n$ analysis windows

To examine the effect of slope calculation at multiple scales this study uses calculated slope from bathymetry data directly using successively larger analysis window sizes. Computations were based on 5 m bathymetry using Landserf software with $n = 5, 7, 9, 21, 49$ and the results are shown in Figure 14. The same colour scale is used allowing direct comparison with the results from other sections. Examination of the slope image at successively large analysis window sizes shows how increasingly larger topographic features are highlighted. At small window sizes steep slopes associated with small topographic variations such as the iceberg ploughmarks are visible. These begin to be blurred by $n = 9$ (ground distance 45 m, 20 m each side of central pixel) and by the time we reach $n = 21$ (ground distance 105 m, 50 m each side of central pixel) it is steep slopes over features of the size of the larger crystalline bedrock structures and larger that are highlighted. By the time we reach $n = 49$ (ground distance 245 m, 120 m each side of central pixel) it is only really the broad slopes on the upper continental shelf that retain high values.

These results are much more similar to those from averaging the bathymetry prior to slope calculation (section 2.2.2, Figure 12) than to those from averaging slope calculations (section 2.2.3, Figure 13) which did not so accurately convey the morphological structure and associated slopes at large window sizes. Multiple scale analysis seems to preserve both fine and broad scale slopes slightly more consistently through increasing analysis window sizes than the previous methods, and provides a method which can be used to match slope analysis scale to the size of geomorphic features we wish to highlight for a particular study. Using Landserf, only window sizes with an odd integer value can be used and a full $n \times n$ cell analysis window is required for a slope value to be computed. Towards the edge of the dataset it becomes increasingly obvious where null values are reported at larger window sizes in Figure 14. This can be a limiting factor in deciding the upper limit of the analysis scale, as can computation time, which increases with analysis window size.

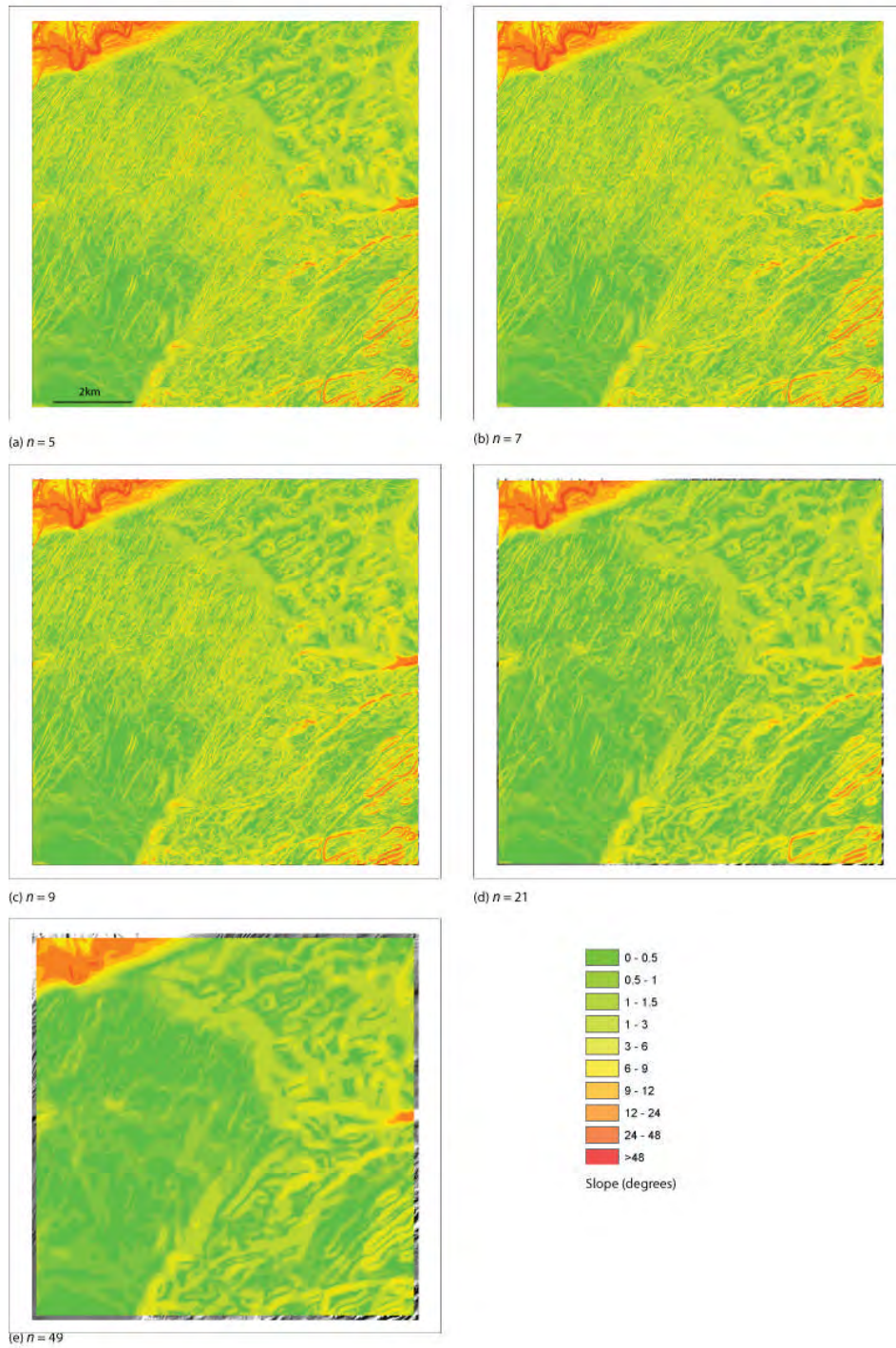


Figure 14. Illustrating the effect of calculating slope from bathymetry data directly using successively larger analysis window sizes. Computations based on 5 m bathymetry using Landserf software with (a) $n = 5$; (b) $n = 7$; (c) $n = 9$; (d) $n = 21$; (d) $n = 49$.

2.2.5 Multiscale analysis

The results of multiscale analysis from the 10 x 10 km study area are shown in Figure 15. This approach seeks to find more of a scale-free slope value by calculating slope across all scales and producing an average of these values. The result seems to be much more successful at retaining geomorphic structure across all scales than averaging over a single scale slope over large window sizes was (Figure 13).

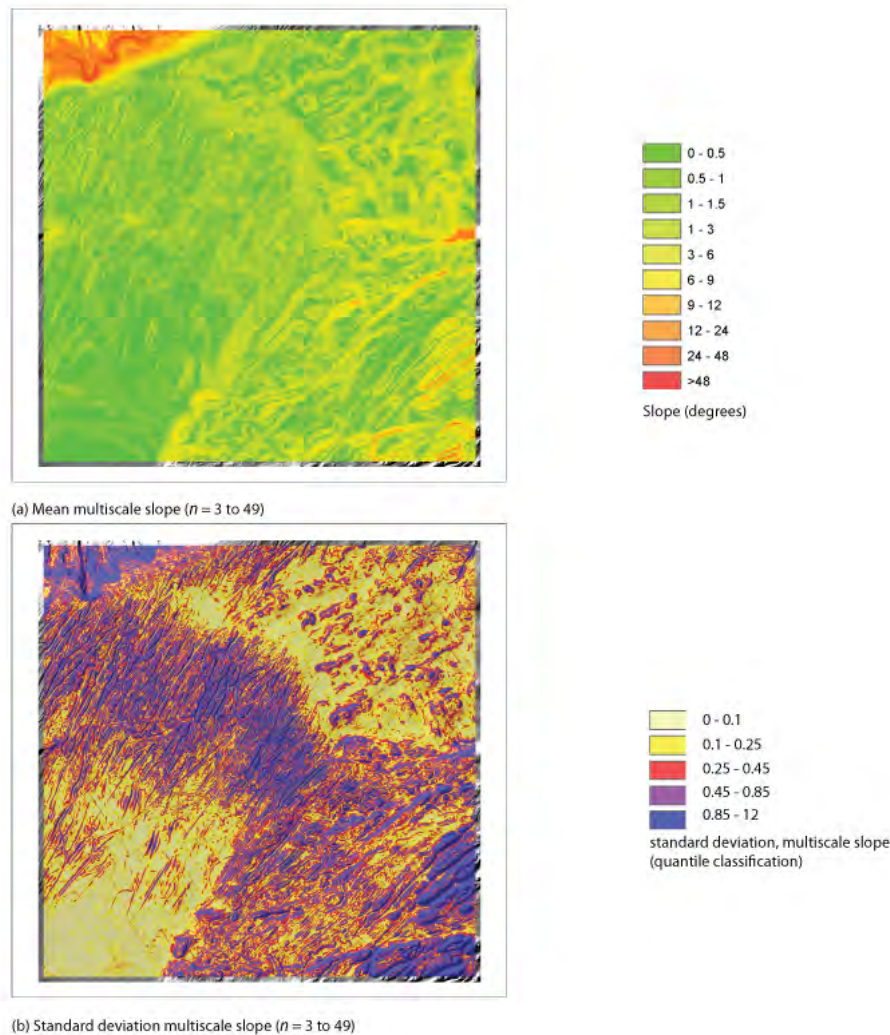


Figure 15. Multiscale slope computed using $N = 49$ (i.e. $n = 3$ to 49). (a) Mean slope over all analysis scales; (b) standard deviation of slope over all analysis scales.

Whilst the high values associated with very small slope features (iceberg ploughmarks) do not retain their high values in the final slope grid it is still perfectly possible to see these small structures and they are seen to have moderately high slopes, which in a regional context is correct. Slopes that have consistently high values over several scales, such as the larger rocky features or the continental slope, appear with the highest values in the multiscale mean slope

grid, but other features that had high values at only certain scales are seen as more moderate slopes. This method seems to give a good general summary of slope, whilst preserving variation in slope associates with structures of different sizes. The multiscale approach to slope calculation also produces an additional dataset which is interesting and may have useful applications. The standard deviation, or variation in slope value across all analysis scales is reported. This gives an indication of how much the topography is changing across multiple scales. Depending on the colour ramp used this may be used to highlight areas of flat or rugged areas across analysis scales (Figure 15b).

If large window sizes are used, particularly on lower resolution grids, null values round the edge of the dataset (due to incomplete $n \times n$ cell window) can be a limiting factor in deciding the upper limit of the analysis scale. Similarly, computation times increase with analysis window size so this is also an important consideration particularly when working with large datasets. Computation of multiscale slope with a maximum window size of $n = 49$ demands significantly more computational resources than a single multiple scale calculation with $n = 49$.

2.3 Other issues related to of slope calculations from bathymetry data

2.3.1 Broad scale slope from Regional data vs. Multibeam data

In the practical context of this study, slope calculations based on regional data are also examined and compared as far as possible with results from multibeam data. This is related to approach 1 (change resolution) in Table 2 but here the focus is more on the differences in the quality of data from different sources at the same nominal resolution. For this part of the study data within the 1000 x 1000 – 10 x 10 km boxes are considered. The main focus is on data within the 100 x 100 km box which allows the best map scale at which to visualise the results between the two bathymetry datasets. Figure 16 shows a simple ArcGIS derived ($n = 3$) slope map produced from the regional 500 m bathymetry dataset. A shaded relief image is shown together with the slope map allowing us to see the topographic structures in more detail and also the artefacts or ‘seams’ in the bathymetry dataset which is a compilation of depth information from a variety of sources. The dataset extends as far as Mohns Ridge, part of the mid-Atlantic ridge system, extending over hundreds of kilometres with a submarine mountain range with peaks rising to thousands of metres from the surrounding deep sea plain.

Features of this size are easily recognisable and the high slopes associated with them are easily captured by the simple slope algorithm, despite the low resolution data. Further towards Norway and the MAREANO area we see how the continental slope appears to be highlighted reasonably well and we can even see details of the some of the banks, channels and canyons off Lofoten-Vesterålen-Senja margin (Thorsnes et al. 2009). Use of larger slope analysis window sizes may help to overcome some of the artefacts and/or focus attention on the larger topographic features as discussed in the next section of this report. However, more important

in this section is to examine how good these regional data really are when we look in more detail. Figure 17 shows the dataset zoomed in to the 100 x 100 km box and compares the data with that from multibeam at nominally the same resolution (i.e. resampled to 500 m). Zooming in further to the 10 x 10 km box is not helpful since we see only pixels in both maps so this is not illustrated.

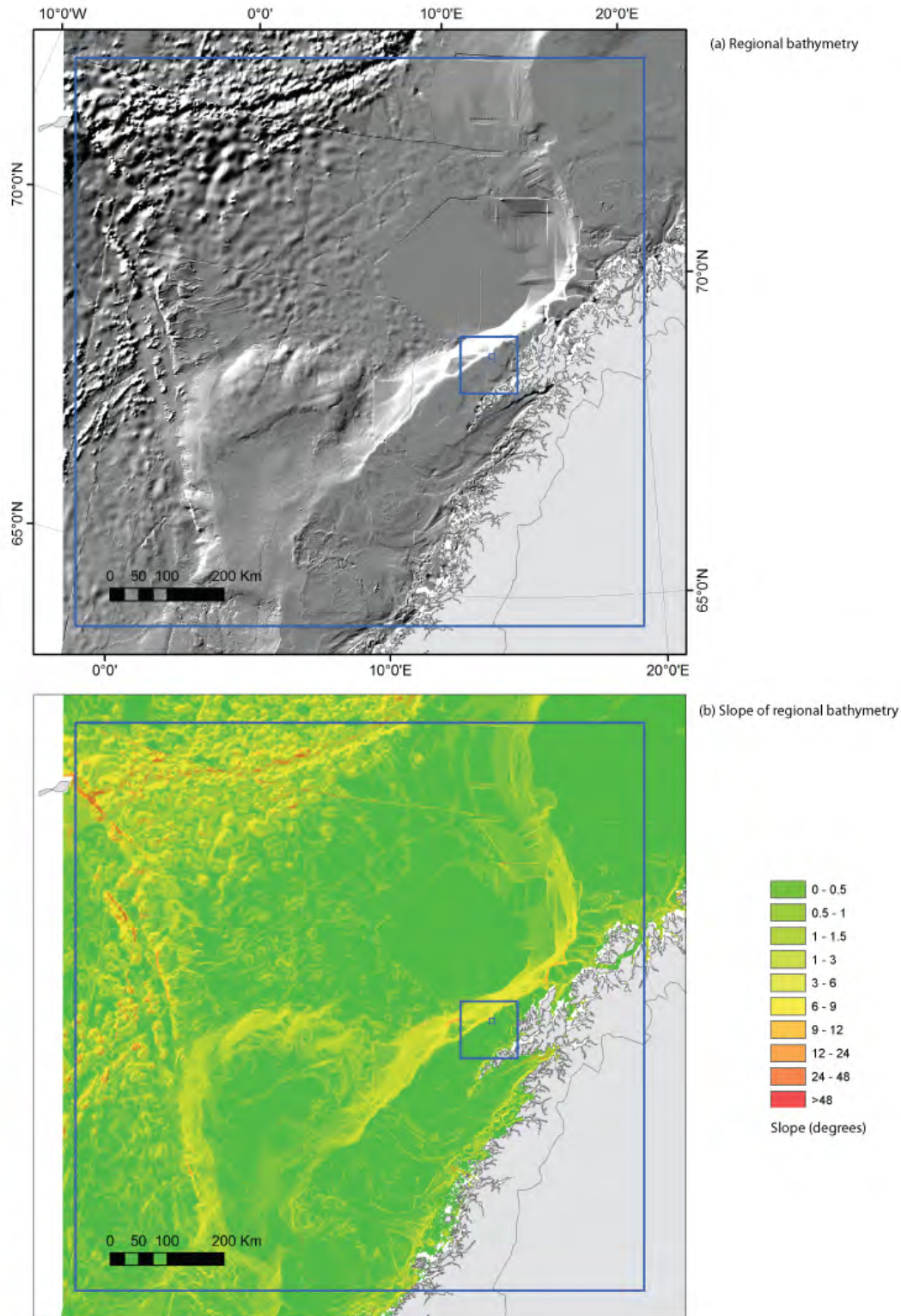


Figure 16: (a) Regional bathymetry 500 m resolution within a 1000 x 1000 km box (b) slope map calculated from regional bathymetry using ArcGIS ($n = 3$)

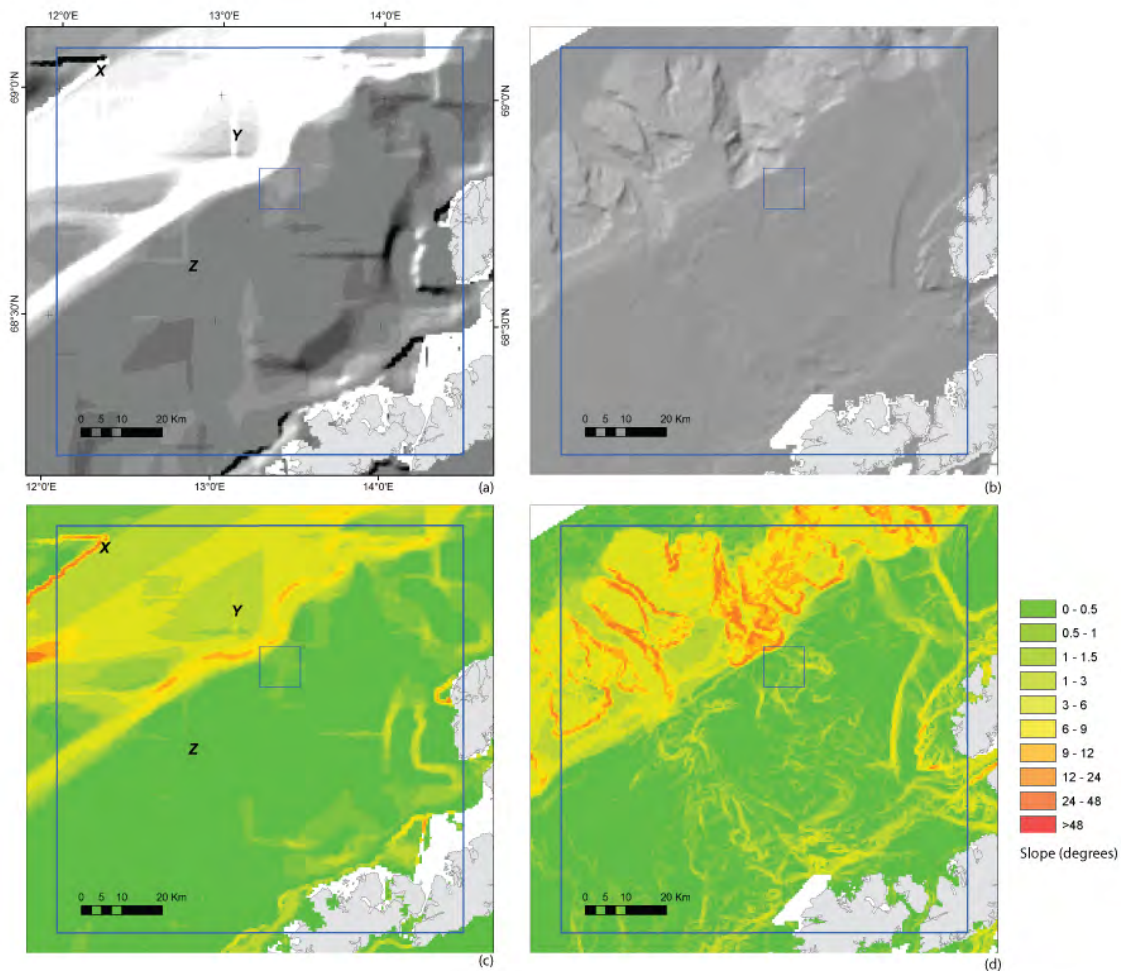


Figure 17. Bathymetry data at 500 m resolution within a 100 x 100 km box, based on (a) regional data (b) multibeam data. Bathymetry data are shown together with derived slope maps calculated in ArcGIS ($n = 3$) (c) slope from regional bathymetry (d) slope from multibeam

Examination of the bathymetry data and derived slope highlights the lack of detail and artefacts in the compiled regional data. The data are sufficient for identification of the continental shelf and slope but beyond this are significantly less detailed in the geomorphology they reveal. This is clearly illustrated in by comparison to multibeam data at the same raster resolution (500 m) which has been down-sampled from higher resolution data with denser bathymetry soundings. Artefacts associated with seams in the compiled dataset are also visible in slope maps generated from the bathymetry (Figure 17c). Approaches 1 to 5 (Table 2) can do little to help this situation but the figures and discussion here has been included here as a cautionary note on the quality of the bathymetry data underlying slope calculations.

2.3.2 Effects of bathymetry data artefacts on slope calculations

Some effects of data artefacts have been shown in the previous section on regional data. Data artefacts are also present in other sources of denser bathymetry data, e.g. Olex bathymetry

(Elvenes et al. 2012) which are prone to more artefacts than multibeam data, yet offer good regional data coverage and basis for slope calculations, at least at broad scales. This section focuses on multibeam data. The quality of multibeam data has improved significantly over the past couple of decades with more sophisticated motion sensors, data acquisition and processing systems allowing many previously troublesome artefacts, such as the motion artefacts described by Hughes Clarke (2003), to be removed. Nevertheless multibeam data is typically built up over a series of years and it is common, in practice, that at least some of the datasets suffer from some kind of artefact, for example related to survey lines, motion residuals, or calibration problems. Using examples from the study area, this section examines how each of the scale approaches (Table 2) help to overcome these artefacts with respect to slope calculations. Data within the 1 x 1 km boxes and neighbouring areas will be used for illustration of typical artefact associated issues.

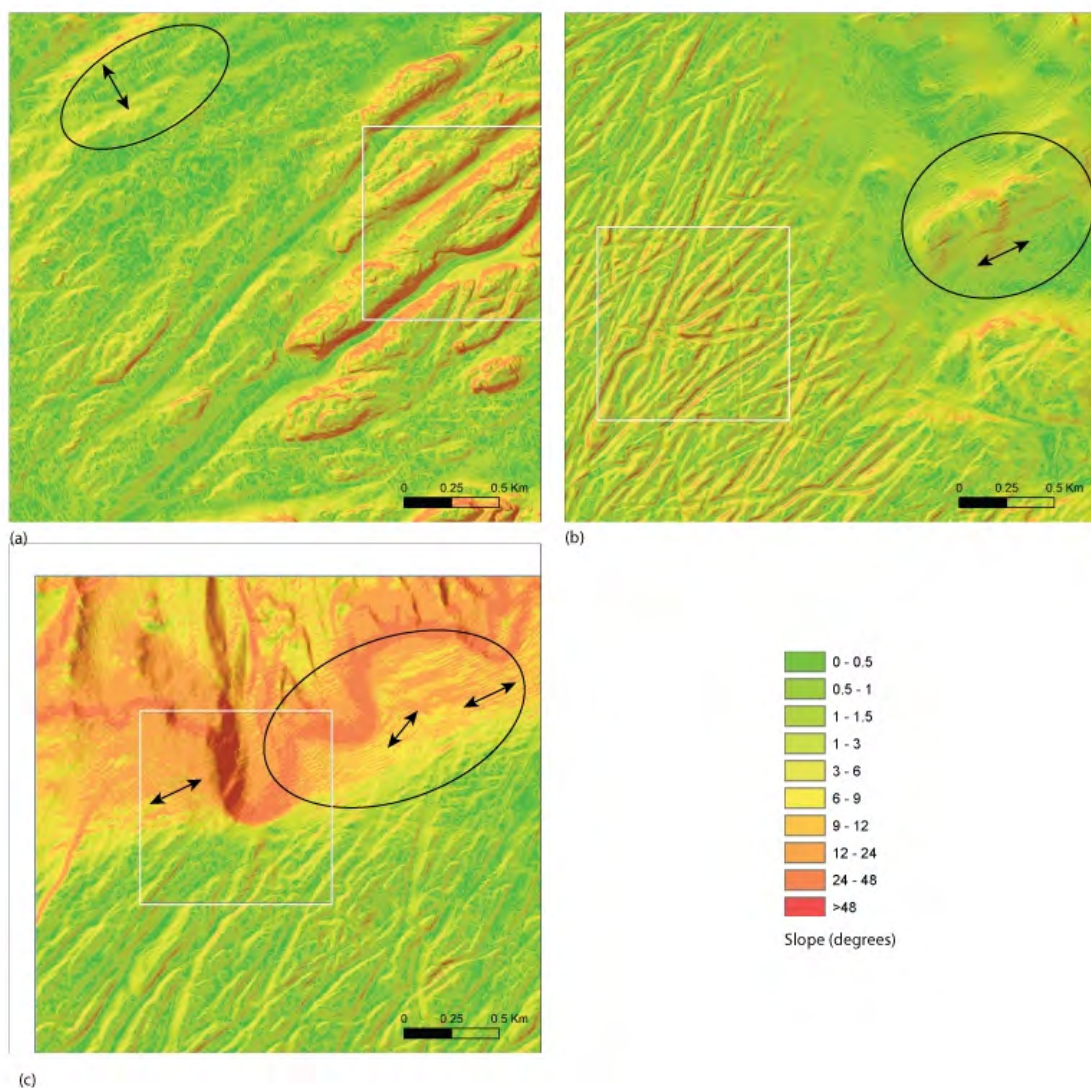


Figure 18. Illustrating artefacts in multibeam data in the vicinity of each 1 x 1 km test site (a) rock, (b) ploughmarks, (c) canyon. Artefacts are visible as strips (corrugations) in the hillshaded bathymetry and are highlighted by erroneous slope values, the orientation of artefacts is indicated at selected locations by double headed arrows.

The artefacts within the study area are quite small by comparison with many other multibeam datasets, however we do see some across-track motion related artefacts, which appear as roughly SW-NE stripes in the slope maps (Figure 18). The black ovals in Figure 18 highlight the artefacts and comparison of the data from each of the 3 test sites shows how the prominence of the artefacts varies across the multibeam dataset. They are almost invisible in the rocky area, but quite obvious in the canyon/upper slope, where the multibeam system is nearing the limits of its depth resolution. Figure 19 shows the extent to which each of the approaches 1-5 (Table 2) help to overcome the artefacts in the slope calculations, using the canyon data as an example, and only selected results for illustrated purposes.

Examination of Figure 19 gives an indication of to what extent each of the approaches from Table 1 helps to overcome artefacts in the multibeam dataset. It can be seen that downsampling the resolution (b), averaging bathymetry or slope over moderate window sizes (c, d) all produce slope images which suffer less than the original calculation (a) from artefacts. Any of these methods may be a good choice for minimising artefacts, depending on the application. The pros and cons of the various methods are discussed elsewhere in this report. Multiple scale analysis reveals that for this dataset an analysis window of 7×7 cells seems to hide most artefacts (e), and successively larger window sizes will further diminish the influence of artefacts. Multiscale analysis offers an alternative means by which to overcome artefacts however the examples shown in (f) shows how smaller multiscale window sizes retain the artefacts longer than their multiple scale counterparts. It can be seen that using $n = 7$ was a large enough window size to overcome most artefacts using the multiple scale approach. When multiscale analysis is used with $n = 3$ to 7 the output includes contributions from 2 smaller window calculations (i.e. $n = 3, 5$) and therefore retains more artefacts, even though both the multi- and multiple scale approaches have the same nominal analysis window size ($n = 7$). Increasing the size of the analysis window further allows for more contributions from slopes computed over larger analysis windows as slope is computed n for all odd integer values up to the specified maximum window size N (i.e. $n = 3, 5, 7, 9, 11, \dots, N$) and we can see from (g) how at large window sizes e.g. $n = 3$ to 49 the effects of artefacts are no longer visible.

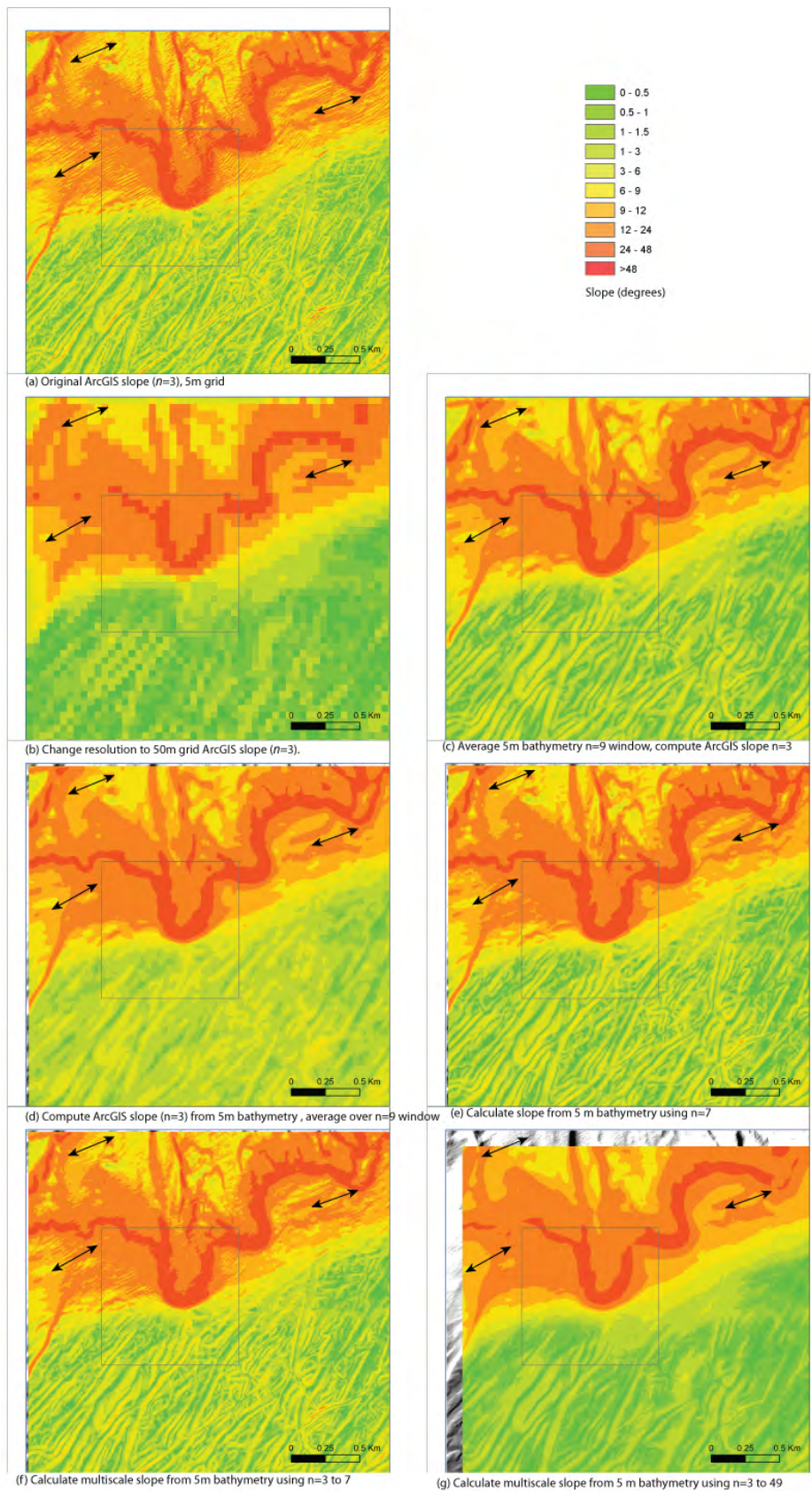


Figure 19. Slope calculations using a selection of approaches from Table 1 to see the effect on overcoming artefacts in the bathymetry dataset. The 1 x 1 km box at the canyon on the upper continental slope (site C – Figure 2) and surrounding neighbourhood are shown. Example artefact locations are indicated by arrows.

2.3.3 Detection of geomorphic structures and relevance to habitats

Slope, along with other terrain variables can provide valuable for the delineation of geomorphic features (Dolan et al. 2012) surficial sediment and habitats (Brown et al. 2011), either directly or by use of modelling methods (e.g. Wilson et al. 2007, Lucieer and Lamarche 2011, Ierodiaconou et al. 2011). Slope has geomorphological relevance since it is intrinsically linked to the shape of topographic features and it is linked to the stability of sediments, determining which grain sizes can maintain their position in relation to the effects of gravity/currents. Slopes are also related to dynamic seabed processes such as the local acceleration or steering of currents which can lead to erosion and transport of sediments, and even the creation of bedforms. Slope is also ecologically relevant, its role in the stability of sediments affects the availability of suitable substrate for particular organisms to live in/on the seabed. Local acceleration of currents around topographic features with sloping sides is linked to food supply, exposure, and other factors which more directly influence an organisms mode of living.

Scale is important to each of these influences on geomorphology and habitat. Table 3 summarises the length scales associated with habitats of different scale, *sensu* Greene et al. (1999) which includes mainly geomorphic classification of habitats at the broader scales. Examples of slope calculations at each of these scales have been shown in the previous sections and the relevant figures are noted in the Table 3. One scale not yet addressed in this report is the finest scale, as in the 100 x 100 m box. An example is shown in Figure 20 showing how slope calculations based on a 5 m grid ($n = 3$) correspond to video-based observations of seabed sediment type from a section of a video transect at site A, the rocky seabed. It can be seen that changes in slope values at this scale and resolution are relevant to video observations. Slope analysis over broader scales, and at coarser grid resolutions can also be relevant to habitat when more video transects are considered together in a regional context (e.g. Dolan et al. 2009, Buhl-Mortensen 2009, Elvenes et al. 2012). For very fine scale mapping closer to the observation scale of video, sub-metre bathymetric grids may be required. In deeper waters this will require mapping from underwater survey platforms (e.g. ROV- Dolan et al. 2008). Further, these studies and others have shown how inclusion of slope and other terrain variables calculated at several analysis scales increases the chance of finding ecologically relevant proxies for environmental parameters affecting the distribution of habitats (species/biotopes). Inclusion of slope and other variables calculated at different scales consequently can improve the results of habitat modelling.

Table 3. Slope feature size detectable within the 100 x 100 m box will depend on data resolution.

Box	Typical Map scale	Figures	Slope feature size	Habitat Scale (Greene et al. 1999)
1000x 1000 km	1:5 000 000	16	>10km	Megahabitat
100 x 100 km	1:500 0 00	17	1 to >10km	Mesohabitat
10 x 10 km	1:50 00 0	9, 12-15	>10 m to 10 km	Meso/Macrohabitat
1 x 1 km	1:5 000	19	>10 m to 1 km	Macrohabitat
100 x 100 m	1:500	20	<1 m to 10 m	Macrohabitat/Microhabitat

Microhabitat will only be resolved by data with sub-metre resolution bathymetry data, e.g. from shallow ship-borne surveys or ROV/AUV based mapping in deeper water.

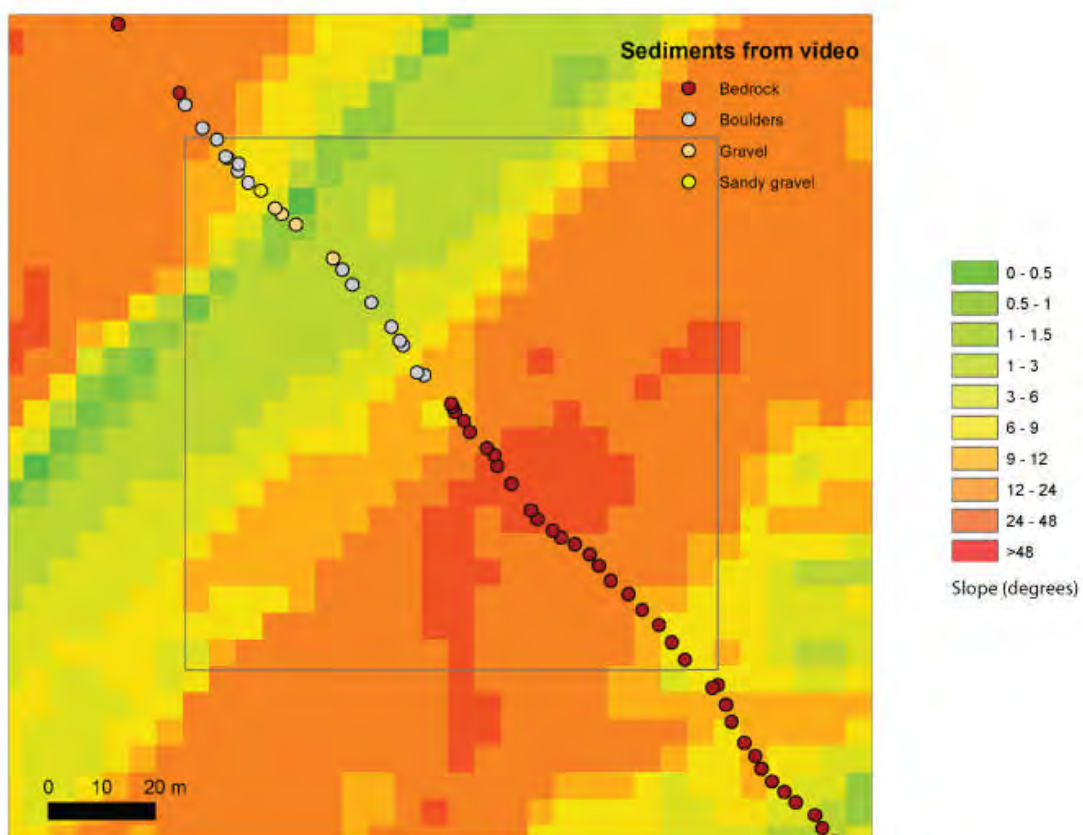


Figure 20. Showing the slope calculated from 5 m resolution bathymetry data using ArcGIS ($n = 3$) within the neighbourhood of a 100 x 100 m box (black) in the rocky study area. Point observations of sediment cover from a towed video transect are overlain on the slope map to show how the variation in sediments (often linked to habitats) varies with slope in this area.

3. DISCUSSION AND CONCLUSIONS

This report has focussed solely on slope as an example terrain variable, however the issues discussed through these examples will be just as important in the computation of other variables. We have seen the power of GIS based calculations and the flexibility they give for analysis at different spatial scales. Compared with more traditional field based methods of computing slope over the length scales of specific topographic features this can give advantages, however it can also lead all too easily to misleading values of slope being reported where insufficient consideration is given to the computation algorithm, data resolution or analysis scale, and the quality of the bathymetric/topographic data underlying slope calculations.

3.1 Computation algorithms

From the analysis of computation algorithms it can be seen that there is some variation in the slope values obtained depending on the method of calculation. This in itself means that the topic is worthy of consideration. Through the examples shown here we see that the effects of using different algorithms vary with data resolution, and with the type/size of feature over which the slope is computed. In practical terms it is fair to say that the majority of GIS users will use only those algorithms available in their own desktop software and will not actively seek out other methods, nonetheless it is important that people are aware of the effect the choice of algorithm can make, and not simply trust 'black box' calculations. The examples shown here extend the suite of algorithms beyond those available from any single software thereby exposing the similarities and differences in the results obtained with different methods and their relative stability over resolution and feature type.

All the computation algorithms considered here use a rectangular analysis window in performing the calculations. Shi et al. (2007) experimented with using a circular neighbourhood for computation of slope. This has not been reproduced in this study as efforts were focussed on examining methods available in common desktop GIS. The authors reported some advantages with the circular neighbourhood, however they also noted that it is more sensitive to noise than a rectangular neighbourhood. This would make it a poor choice for artefact-prone multibeam data. However as bathymetry data quality improves, use of circular or other analysis neighbourhoods could be an alternative worthy of consideration for the future.

3.2 Data resolution/analysis scale

The series of results from the different approaches to data resolution/analysis scale in section 2.2 have shown that there is a good deal of variation in the slope values obtained. This study has therefore highlighted considerations related to this topic which should be borne in mind by those conducting slope analyses of bathymetry or similar data, so they can make an informed choice as to the best approach. Several papers in the terrestrial literature have previously compared approaches to computation of terrain variables including slope with regard for data resolution/analysis scale (e.g. Albani et al. 2004, Gao et al. 2012, Zhu et al 2008) and some have made recommendations as to the best approach, usually focussing on a particular application e.g. soil science, geohazards. For example Hodgson (1995) recommend not to resample elevation data to coarser grids but to find mean slope in larger window for each larger cell size. Results of this study illustrate more approaches to slope computation at different scales than some of the other studies in order to provide a broad illustration of the issues surrounding the topic, while several of the other studies have focussed on detailed analysis of one particular approach.

A general rule for the best method is difficult to recommend since it will depend on the purpose of the analysis and the quality/resolution of available bathymetry data. This study provides a detailed illustration of the effects of the various approaches (Table 2) and highlighting issues GIS users should consider when selecting their approach to slope calculation. The average slope method should be used with caution since it differs from the general picture presented by other methods. However this approach may be useful and the most appropriate method in certain situations, especially at only small-moderate window sizes. For example for standardising the area of seabed under analysis to that observed by other methods, e.g. video data (Dolan et al. 2009, Elvenes, 2012). The fact that averaging slope highlights a whole area where high, fine scale slope values occur may be more useful than just identifying areas of broader slopes, which the other approaches to calculating scale at different scales produce.

Each of the 5 approaches to characterising the terrain at multiple scales (Table 2) offers new information. Each somehow provide a means to examine slope over different length scales, be this by varying resolution, or the extent of the area considered for terrain analysis. Several of the approaches also involve production of null values or edge effects with spurious data round the edges of the bathymetric data coverage. The importance of this will always be a trade off in the context of any particular study. For example, mapping in narrow fjords will lose too much data if large analysis windows are used, so methods that minimise this effect will be preferable. Nevertheless, GIS users should be mindful of potential edge effects induced by other slope calculation methods which seemingly give a result right to the edge of the bathymetry dataset, as we have seen in Section 2.

3.3 Other issues

This study included a brief look at slope calculations based on regional, compiled bathymetry datasets, and compared the results with slope calculations based on multibeam data at nominally the same grid resolution, and at finer resolutions. It is clear that data quality is an important issue, not just data resolution. We have seen how certain regional datasets are prone to artefacts resulting from the compilation process, however we have also seen how broad-scale geomorphic features and their associated slopes emerge from the data nonetheless. The suitability of a dataset for any particular type of study will always be a judgement call by the investigating scientist and will be influenced largely by the options for available data.

Multibeam data acquisition is costly and time consuming, whilst regional datasets are adequate for many purposes including geomorphology and habitat mapping at a regional scale (e.g. case study using 500 m data in Dolan et al. 2012). The effect of some typical data artefacts in bathymetry data has been illustrated. Other datasets will have different artefacts, for example survey-line to survey-line discontinuities, however assuming the data have been processed to the best possible standard the issues surrounding slope calculation, or that of other terrain variables will be similar to those presented here.

This report has focussed on three indicative scales of data resolution/mapping, and these are the same as examined in a recent report for the European Geo-Seas project (Dolan et al, 2012) to which this report provides a more in depth support on one example of a variable from terrain analysis. The demand exists already for pan-European seabed maps, a fact borne out by projects and initiatives such as Marine Knowledge 2020, EMODNET and Geo-Seas. Standardisation of data resolutions (with due regard to data quality/density) and mapping scales are key concepts that will help such programmes move forward. It is also important that terrain analysis of slope and other variables, is performed in an informed manner, with due regard for computation algorithms, data resolution and analysis scale.

This report has highlighted the differences in computed values of slope arising from each of these influences. The very fact that differences exist should be proof enough that GIS based calculations should not be taken at face value. Documentation of computation algorithm, data resolution and analysis should support computed slope values, or slope image grids such that the reader can interpret the value presented in an informed manner.

3.4 Conclusion

The clearest take home message from this study is that the results presented here have demonstrated that the value of slope (degrees) for any particular location will vary depending on computation algorithm, data resolution and analysis scale. It is therefore essential that slope values are reported together with details of their computation in terms of these three key influences. X degrees slope on a map or report means nothing if the reader does not know

how the computation was performed. It is difficult to offer advice on the best method for computation algorithm, for data resolution or for analysis scale. The purpose of this study was simply to perform a comprehensive test and illustrate the effects of these issues on slope calculations, thereby raising awareness of the issues.

A judgement call as to the best method should be made by scientists when using slope, or other terrain variable, from bathymetric or other topographic data given a particular set of data or research objective. Once this decision has been made, it is important that the results are fully documented so that readers know which methods have been used.

4. REFERENCES

- Albani, M., B. Klinkenberg, D. W. Anderson & J. P. Kimmins (2004) The choice of window size in approximating topographic surfaces from digital elevation models. *International Journal of Geographical Information Science*, 18, 577-593
- Bauer, J., Rohdenburg, H., Bork, H. R. (1985). *Ein digitales reliefmodell als voraussetzung fuer ein deterministisches modell der wasser- und stoff-fluess, landschaftsgenese und landschaftsoekologie, h.10, parameteraufbereitung fuer deterministische gebiets-wassermodelle, grundlagenarbeiten zu analyse von agrar-oekosystemen* (Eds.: Bork, H.-R.; Rohdenburg, H.), pp 1-15 [In German].
- Brown, C. J., S. J. Smith, P. Lawton & J. T. Anderson (2011) Benthic habitat mapping: A review of progress towards improved understanding of the spatial ecology of the seafloor using acoustic techniques. *Estuarine Coastal and Shelf Science*, 92, 502-520.
- Buhl-Mortensen, P., Dolan, M., Buhl-Mortensen, L. (2009): Prediction of benthic biotopes on a Norwegian offshore bank using a combination of multivariate analysis and GIS classification. *ICES Journal of Marine Science*, 66, 2026–2032
- Costa-Cabral, M. C., Burges, S. J. (1994). Digital elevation model networks (DEMON): a model of flow over hillslopes for computation of contributing and dispersal areas. *Water Resources Research* 30, 1681–92.
- Dolan, M. F. J., P. Buhl-Mortensen, T. Thorsnes, L. Buhl-Mortensen, V. K. Bellec & R. Boe (2009) Developing seabed nature-type maps offshore Norway: initial results from the MAREANO programme. *Norwegian Journal of Geology*, 89, 17-28.
- Dolan, M.F.J.; Thorsnes, T.; Leth, J.; Alhamdani, Z.; Guinan, J.; Van Lancker, V. (2012). Terrain characterization from bathymetry data at various resolutions in European waters - experiences and recommendations. *NGU Report.2012.045*.
- Dragut, L., T. Schauppenlehner, A. Muhar, J. Strobl & T. Blaschke (2009) Optimization of scale and parametrization for terrain segmentation: An application to soil-landscape modeling. *Computers & Geosciences*, 35, 1875-1883.
- Dunn, M. & R. Hickey. (1998). The Effect of Slope Algorithms on Slope Estimates within a GIS. *Cartography* 27, 9-15.
- Elvenes, Buhl-Mortensen & Dolan (2012) Evaluation of alternative bathymetry data sources for MAREANO: A comparison of Olex and multibeam data for substrate and biotope mapping. *NGU report 2012-030*.

- Evans, I. S. (1972). General geomorphometry, derivatives of altitude, and descriptive statistics. In *Spatial Analysis in Geomorphology*, ed. R. J. Chorley, pp17–90. London: Methuen.
- Evans, I.S. (1980) An integrated system of terrain analysis and slope mapping. *Zeitschrift für Geomorphologic, Suppl-Bd 36*, 274-295.
- Evans, I.S. (2012) Geomorphometry and landform mapping: What is a landform? *Geomorphology*, 137, 94-106.
- Florinsky, I. V. (1998a) Accuracy of local topographic variables derived from digital elevation models. *International Journal of Geographical Information Science*, 12, 47-61.
- Florinsky, I.V. (1998b) Combined analysis of digital terrain models and remotely sensed data in landscape investigations. *Progress in Physical Geography*, 22, 33-60.
- Gao, J., J. E. Burt & A. X. Zhu (2012) Neighborhood size and spatial scale in raster-based slope calculations. *International Journal of Geographical Information Science*, 1-20. *In press*. DOI:10.1080/13658816.2012.657201.
- García Rodríguez, J. L. & M. C. Giménez Suárez. (2010). Comparison of mathematical algorithms for determining the slope angle in GIS environment.. *Aqua-LAC: UNESCO*, 2(2), 78-82.
- Greene, H. G., M. M. Yoklavich, R. M. Starr, V. M. O’Connell, W. W. Wakefield, D. E. Sullivan, J. E. McRea, Jr., and G. M. Cailliet. (1999). A classification scheme for deep seafloor habitats. *Oceanologica Acta*, 22, 663–678.
- Grohmann, C. H., M. J. Smith & C. Riccomini (2011) Multiscale Analysis of Topographic Surface Roughness in the Midland Valley, Scotland. *IEEE Transactions on Geoscience and Remote Sensing*, 49,1200-1213.
- Haralick, R. M. (1983). Pattern recognition and classification. *Manual of Remote Sensing*, 2nd Edition, Vol. 1, Ch.18, American Society of Photogrammetry.
- Heerdegen, R.G. & Beran, M.A. (1982). Quantifying Source Areas Through Land Surface Curvature and Shape. *Journal of Hydrology*. 57: 359-373.
- Hickey, R. (2000) Slope Angle and Slope Length Solutions for GIS. *Cartography*, 29, 1-8.
- Hickey, R, A. Smith, AND P. Jankowski. (1994). Slope length calculations from a DEM within ARC/INFOGRID: *Computers, Environment and Urban Systems*, v. 18, 5, pp. 365 - 380.

Hodgson, M. E. (1995) What cell-size does the computed slope aspect angle represent. *Photogrammetric Engineering and Remote Sensing*, 61, 513-517.

Horn, B.K.P. (1981) Hill shading and the reflectance map. *Proceedings of the IEEE* 69(1), 14 – 47. Hughes Clarke, J. E. (2003) Dynamic motion residuals in swath sonar data: Ironing out the creases. *International Hydrographic Review*, 4, 6-23.

Ierodiaconou, D., J. Monk, A. Rattray, L. Laurenson & V. L. Versace (2011) Comparison of automated classification techniques for predicting benthic biological communities using hydroacoustics and video observations. *Continental Shelf Research*, 31, S28-S38.

IOC, IHO & BODC. (2003). *Centenary Edition of the GEBCO Digital Atlas*. Liverpool: published on CD ROM on behalf of the Intergovernmental Oceanographic Commission and the International Hydrographic Organization as part of the General Bathymetric Chart of the Oceans, British Oceanographic Data Centre.

Jenness, J. (2011). DEM Surface Tools v. 2.1.292. Jenness Enterprises. Available at: http://www.jennessent.com/arcgis/surface_area.htm.

Jones, K. H. (1998) A comparison of algorithms used to compute hill slope as a property of the DEM. *Computers & Geosciences*, 24, 315-323.

Lucieer, V. & G. Lamarche (2011) Unsupervised fuzzy classification and object-based image Analysis of multibeam data to map deep water substrates, Cook Strait, New Zealand. *Continental Shelf Research*, 31, 1236-1247.

Olaya V. (2011) SEXTANTE for ArcGIS. http://gvsigce.sourceforge.net/sextante_web/arcgis.html

Pickrill, R. A. & B. J. Todd (2003) The multiple roles of acoustic mapping in integrated ocean management, Canadian Atlantic continental margin. *Ocean & Coastal Management*, 46, 601-614.

Sharpnack, D. A. and Akin, G. (1969) An algorithm for computing slope and aspect from elevations. *Photogrammetric Engineering* 35(3), 247 – 248.

Shary, P. A., L. S. Sharaya & A. V. Mitusov (2002) Fundamental quantitative methods of land surface analysis. *Geoderma*, 107, 1-32.

Shi, X., A. X. Zhu, J. Burt, W. Choi, R. X. Wang, T. Pei, B. L. Li & C. Z. Qin (2007) An experiment using a circular neighborhood to calculate slope gradient from a DEM. *Photogrammetric Engineering and Remote Sensing*, 73, 143-154.

Tarboton, D.G. & Shankar, U. (1997). The identification and mapping of flow networks from digital elevation data. Invited Presentation at AGU Fall Meeting. San Francisco. USA

Thorsnes, T., L. Erikstad, M. F. J. Dolan & V. K. Bellec (2009) Submarine landscapes along the Lofoten Vesteralen-Senja margin, northern Norway. *Norwegian Journal of Geology*, 89, 5-16.

Travis, M.R., Elsner, G.H., Iverson, W.D., Johnson, C.G. (1975). VIEWIT computation of seen areas, slope, aspect for land use planning. US Dept. of Agricultural Forest Service Technical report PSW 11/1975, Pacific Southwest Forest and Range Experimental Station, Berkley, California. USA

Warren, S. D., M. G. Hohmann, K. Auerswald & H. Mitsova (2004) An evaluation of methods to determine slope using digital elevation data. *Catena*, 58, 215-233.

Wilson, J. P. (2012) Digital terrain modeling. *Geomorphology*, 137, 107-121.

Wilson, M. F. J., B. O'Connell, C. Brown, J. C. Guinan & A. J. Grehan (2007) Multiscale Terrain Analysis of Multibeam Bathymetry Data for Habitat Mapping on the Continental Slope. *Marine Geodesy*, 30, 3-35.

Wood, J. (2009). Landserf Version 2.3 (www.landserf.org).

Zevenbergen, L. W. & C. Thorne (1987) Quantitative analysis of land surface topography. *Earth Surface Processes and Landforms*, 12, 47-56.

Zhang, X., N. A. Drake, J. Wainwright & M. Mulligan (1999) Comparison of slope estimates from low resolution DEMs: Scaling issues and a fractal method for their solution. *Earth Surface Processes and Landforms*, 24, 763-779.

Zhu, A.-X., J. E. Burt, M. Smith, R. Wang & J. Gao. (2008). The Impact of Neighbourhood Size on Terrain Derivatives and Digital Soil Mapping. *Advances in Digital Terrain Analysis*. eds. Q. Zhou, B. Lees & G.-a. Tang, 333-348. Springer Berlin Heidelberg.



Norges geologiske undersøkelse
Postboks 6315, Sluppen
7491 Trondheim, Norge

Besøksadresse
Leiv Eirikssons vei 39, 7040 Trondheim

Telefon 73 90 40 00
Telefax 73 92 16 20
E-post ngu@ngu.no
Nettside www.ngu.no

*Geological Survey of Norway
PO Box 6315, Sluppen
7491 Trondheim, Norway*

*Visitor address
Leiv Eirikssons vei 39, 7040 Trondheim*

*Tel (+ 47) 73 90 40 00
Fax (+ 47) 73 92 16 20
E-mail ngu@ngu.no
Web www.ngu.no/en-gb/*